particles were immunogenic and that insertion of a tag into the E2 protein could induce antibodies as a secondary immunogen.

4. Discussion

In this study we showed that infectious FLAG-tagged HCV particles with an N151K mutation that modulated HCV-glycosylation could be efficiently produced in cells and purified on a FLAG-agarose column. This purification procedure allowed analysis of the physical properties of the particles and the generation of anti-E2 antibodies.

The FLAG-tagged HCV particles were purified by simple anti-FLAG affinity chromatography in combination with ultrafiltration. However, the efficiency of purification was low, and the recovery of the HCV core protein in the final purified virus preparation was only approximately 5%. This low efficiency of purification of the HCV particles maybe due to a number of factors: (1) Interaction between the E2-FLAG protein and the anti-FLAG-agarose column may have been prevented by cellular host proteins with specific or non-specific affinity for the anti-FLAG-agarose, (2) A conformation change may have occurred in the E2 protein due to insertion of the FLAG sequence, which may have blocked FLAG interaction with anti-FLAG, (3) Free FLAG-E2 proteins may have bound more tightly to the FLAG-agarose than the FLAG-E2 protein on the viral surface. Nevertheless, sufficient purified FLAG-HCV particles were obtained with this purification procedure for further analysis.

In the density gradient analysis of the purified HCV particles, the peak of the HCV core protein coincided with the peaks of HCV RNA and viral infectivity. In previous reports of density gradient fractionation of non-FLAG-tagged viral particles, the peak of infectivity was reported to shift to a lighter density fraction than the peaks of HCV core protein or RNA [8,13,14]. This discrepancy between our, and previous, data may be explained by the fact that the properties of the purified FLAG-tagged HCV particles may differ from those of the JFH-1 based HCV particles reported previously. Regarding viral infectivity, it is known that cholesterol and sphingolipid association with HCV particles is important for virion maturation and infectivity [9]. The association of HCV particles with these lipids occurs in lipid rafts [9]. Since the E2-FLAG protein may have a decreased dependency on lipid rafts compared to the non-tagged E2 protein, this therefore resulted in a shift in the peak of infectivity. Alternatively, an association between HCV and very-low-density lipoprotein (VLDL) has an important role in HCV infectivity [15]. Tagging of HCV particles with FLAG may have somehow changed the association of HCV with VLDL and cause the observed shift in the infectivity peak. The mechanism of the shift of the infectivity peak of the FLAG-HCV particles needs to be examined in more detail in future studies.

HCV particles from human plasma samples have been previously examined by immunogold electron microscopy [16]. In the present study, we could clearly observe spherical particle structures of 40–60 nm in the purified samples. Furthermore, the FLAG-tagged HCV particles were aggregated by anti-FLAG antibody. This is the first report of the aggregation of HCV particles produced in an *in vitro* culture system. This method may therefore facilitate future examination of the detailed conformation of HCV particles and future elucidation of HCV particle structure by cryo-electron microscopy. However, it is regarded structural analysis as difficult to that aggregated HCV particles were inequable showing in this report because of this method also gathered defective viral particles which have the E2-FLAG protein.

Immunization of mice with purified FLAG-tagged HCV particles induced anti-E2 as well as anti-FLAG antibodies. These results indicated that the envelope proteins of the FLAG-tagged HCV particles were immunogenic and that insertion of a tag into the E2 protein could induce antibodies as a secondary immunogen. Thus, not only epitopes of viral origin, but also an epitope inserted into the virus, can induce an immune response. Although it is unclear how many amino acids can be inserted into the E2 HVR1, at least a triple FLAG-tag sequence (25 amino acids) is possible as shown in this study.

In conclusion, we have established a simple system for the purification of recombinant infectious FLAG-epitope-tagged HCV particles. The use of this system may contribute to studies aimed at a detailed analysis of HCV particle structure and towards HCV vaccine development.

Acknowledgments

This work was partially supported by a grant-in-aid for Scientific Research from the Japan Society for the Promotion of Science, from the Ministry of Health, Labor and Welfare of Japan, by the Research on Health Sciences Focusing on Drug Innovation from the Japan Health Sciences Foundation, and by the Japanese Society of Gastroenterology.

References

[1] K. Shimotohno, Hepatitis C virus as a causative agent of hepatocellular carcinoma, Intervirology 38 (1995) 162–169.
[2] Q.L. Choo, K.H. Richman, J.H. Han, K. Berger, C. Lee, C. Dong, C. Gallegos, D. Coit, R. Medina-Selby, P.J. Barr, A.J. Weiner, D.W. Bradley, G. Kuo, M. Houghton, Genetic organization and diversity of the hepatitis C virus, Proc. Natl. Acad. Sci. USA 88 (1991) 2451–2455.
[3] N. Kato, M. Hijikata, Y. Ootsuyama, M. Nakagawa, S. Ohkoshi, T. Sugimura, K. Shimotohno, Molecular cloning of the human hepatitis C virus genome from Japanese patients with non-A, non-B hepatitis, Proc. Natl. Acad. Sci. USA 87 (1990) 9524–9528.
[4] Z. Stamataki, S. Coates, M.J. Evans, M. Wininger, K. Crawford, C. Dong, Y.L. Fong, D. Chien, S. Abrignani, P. Balfe, C.M. Rice, J.A. McKeating, M. Houghton, Hepatitis C virus envelope glycoprotein immunization of rodents elicits cross-reactive neutralizing antibodies, Vaccine 25 (2007) 7773–7784.
[5] T. Kato, T. Date, M. Miyamoto, A. Furusaka, K. Tokushige, M. Mizokami, T. Wakita, Efficient replication of the genotype 2a hepatitis C virus subgenomic replicon, Gastroenterology 125 (2003) 1808–1817.
[6] T. Wakita, T. Pietschmann, T. Kato, T. Date, M. Miyamoto, Z. Zhao, K. Murthy, A. Habermann, H.G. Krausslich, M. Mizokami, R. Bartenschlager, T.J. Liang, Production of infectious hepatitis C virus in tissue culture from a cloned viral genome, Nat. Med. 11 (2005) 791–796.
[7] J. Zhong, P. Gastaminza, G. Cheng, S. Kapadia, T. Kato, D.R. Burton, S.F. Wieland, S.L. Uprichard, T. Wakita, F.V. Chisari, Robust hepatitis C virus infection in vitro, Proc. Natl. Acad. Sci. USA 102 (2005) 9294–9299.
[8] B.D. Lindenbach, M.J. Evans, A.J. Syder, B. Wolk, T.L. Tellinghuisen, C.C. Liu, T. Maruyama, R.O. Hynes, D.R. Burton, J.A. McKeating, C.M. Rice, Complete replication of hepatitis C virus in cell culture, Science 309 (2005) 623–626.
[9] H. Aizaki, K. Morikawa, M. Fukasawa, H. Hara, Y. Inoue, H. Tani, K. Saito, M. Nishijima, K. Hanada, Y. Matsuura, M.M. Lai, T. Miyamura, T. Wakita, T. Suzuki, Critical role of virion-associated cholesterol and sphingolipid in hepatitis C virus infection, J. Virol. 82 (2008) 5715–5724.
[10] M.J. van den Hoff, A.F. Moorman, W.H. Lamers, Electroporation in 'intracellular' buffer increases cell survival, Nucleic Acids Res. 20 (1992) 2902.
[11] T. Takeuchi, A. Katsume, T. Tanaka, A. Abe, K. Inoue, K. Tsukiyama-Kohara, R. Kawaguchi, S. Tanaka, M. Kohara, Real-time detection system for quantification of hepatitis C virus genome, Gastroenterology 116 (1999) 636–642.
[12] D. Delgrange, A. Pillez, S. Castelain, L. Cocquerel, Y. Rouille, J. Dubuisson, T. Wakita, G. Duverlie, C. Wychowski, Robust production of infectious viral particles in Huh-7 cells by introducing mutations in hepatitis C virus structural proteins, J. Gen. Virol. 88 (2007) 2495–2503.
[13] D. Akazawa, T. Date, K. Morikawa, A. Murayama, N. Omi, H. Takahashi, N. Nakamura, K. Ishii, T. Suzuki, M. Mizokami, H. Mochizuki, T. Wakita, Characterization of infectious hepatitis C virus from liver-derived cell lines, Biochem. Biophys. Res. Commun. 377 (2008) 747–751.
[14] Y. Miyanari, K. Atsuzawa, N. Usuda, K. Watashi, T. Hishiki, M. Zayas, R. Bartenschlager, T. Wakita, M. Hijikata, K. Shimotohno, The lipid droplet is an important organelle for hepatitis C virus production, Nat. Cell Biol. 9 (2007) 1089–1097.
[15] S.U. Nielsen, M.F. Bassendine, A.D. Burt, C. Martin, W. Pumeechockchai, G.L. Toms, Association between hepatitis C virus and very-low-density lipoprotein (VLDL)/LDL analyzed in iodixanol density gradients, J. Virol. 80 (2006) 2418–2428.
[16] M. Kaito, S. Watanabe, H. Tanaka, N. Fujita, M. Konishi, M. Iwasa, Y. Kobayashi, E.C. Gabazza, Y. Adachi, K. Tsukiyama-Kohara, M. Kohara, Morphological identification of hepatitis C virus E1 and E2 envelope glycoproteins on the virion surface using immunogold electron microscopy, Int. J. Mol. Med. 18 (2006) 673–678.

Antiviral Research 85 (2010) 520–524

Contents lists available at ScienceDirect

Antiviral Research

journal homepage: www.elsevier.com/locate/antiviral

Identification of hepatitis C virus genotype 2a replicon variants with reduced susceptibility to ribavirin

Su Su Hmwe[a,b], Hideki Aizaki[a], Tomoko Date[a], Kyoko Murakami[a], Koji Ishii[a], Tatsuo Miyamura[a], Kazuhiko Koike[b], Takaji Wakita[a], Tetsuro Suzuki[a,*]

[a] Department of Virology II, National Institute of Infectious Diseases, 1-23-1 Toyama, Shinjuku-ku, Tokyo 162-8640, Japan
[b] Department of Gastroenterology, Graduate School of Medicine, University of Tokyo, 7-3-1 Hongo, Bunkyo-ku, Tokyo 113-8655, Japan

ARTICLE INFO

Article history:
Received 8 April 2009
Received in revised form 19 October 2009
Accepted 18 December 2009

Keywords:
Hepatitis C virus
Replication
Ribavirin
Drug resistance

ABSTRACT

Ribavirin (RBV), a nucleoside analogue, is used in the treatment of hepatitis C virus (HCV) infection in combination with interferons. However, potential mechanisms of RBV resistance during HCV replication remain poorly understood. Serial passage of cells harboring HCV genotype 2a replicon in the presence of RBV resulted in the reduced susceptibility of the replicon to RBV. Transfection of fresh cells with RNA from RBV-resistant replicon cells demonstrated that the RBV resistance observed is largely replicon-derived. Four major amino acid substitutions: T1134S in NS3, P1969S in NS4B, V2405A in NS5A, and Y2471H in NS5B region, were identified. Site-directed mutagenesis of these mutations into the replicon indicated that Y2471H plays a role in the reduced susceptibility to RBV and leads to decrease in replication fitness. The results, in addition to analysis of sequence database, suggest that HCV variants with reduced susceptibility to RBV identified are preferential to genotype 2a.

1. Introduction

Hepatitis C virus (HCV) is a leading cause of chronic liver diseases, such as chronic hepatitis, cirrhosis and hepatocellular carcinoma, affecting approximately 170 million people worldwide (WHO, 2000). HCV belongs to the genus Hepacivirus of the family Flaviviridae, and its genome is a single-stranded, positive-sense RNA of 9.6 kb. HCV displays marked genetic heterogeneity and is currently classified into 6 major genotypes and more than 50 subtypes. HCV genotypes have regional distribution and, of those, genotypes 1 and 2 are detected worldwide (Simmonds et al., 2000). Current standard therapy for chronic hepatitis C consists of the combination of pegylated interferon alpha (IFN-α) in combination with ribavirin (RBV). However, approximately 50% of treated patients infected with genotype 1 do not respond or show only a partial or transient response and treatment is limited by the adverse effects of both agents (Manns et al., 2001; Fried et al., 2002).

HCV replication is associated with a high rate of mutation that gives rise to a mixed and changing population of mutants, known as quasispecies (Martell et al., 1992; Domingo, 1996). The characteristic of HCV may have important implications concerning viral persistence, pathogenicity and resistance to antiviral agents (Domingo, 1996; Forns et al., 1999; Farci and Purcell, 2000). Most previous studies on the possible relationship between HCV quasispecies and response to chemotherapy have been carried out in HCV genotype 1 patients. In addition, several studies have successfully demonstrated that the HCV subgenomic replicon is derived from genotype 1, which typically contains HCV nonstructural genes placed downstream of the neomycin phosphotransferase gene, in selecting variants resistant to antiviral inhibitors. Two studies have demonstrated the identification of HCV genotype 1 mutants responsible for decreased sensitivity to RBV (Young et al., 2003; Pfeiffer and Kirkegaard, 2005). However, little is known about the generation of genotype 2 isolates resistant to antivirals including RBV, or the molecular mechanisms that confer resistance.

In this study, we report the generation and characterization of HCV genotype 2a replicon variants with reduced susceptibility to RBV. The impacts of major amino acid substitutions observed on RBV susceptibility and viral replication capacity were also examined.

2. Materials and methods

2.1. Compounds

RBV and IFN-α were purchased from MP Biomedicals (Eschwege, Germany) and Dainippon Sumitomo Pharma (Osaka, Japan), respectively.

* Corresponding author. Tel.: +81 3 5285 1111; fax: +81 3 5285 1161.
E-mail address: tesuzuki@nih.go.jp (T. Suzuki).

0166-3542/$ – see front matter © 2010 Elsevier B.V. All rights reserved.
doi:10.1016/j.antiviral.2009.12.008

Table 1
Primers used for PCR and nucleotide sequencing.

Region	Primer name	Nucleotide sequence	Position[a]	Polarity
NS3–4A–4B region	PCR primers			
	JF1S	GAAAAACACGATGATACCATG	1756–1776	Sense
	JF1AS	AACCCAGTCCCACACGTC	4650–4633	Antisense
	Sequencing primers			
	JF5S	CACTTTCAGTGACAACAGCA	2322–2341	Sense
	JF6S	CGCCACCGACGCCCTCATGA	3003–3022	Sense
	JF4AS	CTGGTCGACAACGGACTGGT	4109–4090	Antisense
NS5A–NS5B region	PCR primers			
	JF2S	TGCTCCGGATCCTGGCTC	4612–4629	Sense
	JF2AS	TACCTAGTGTGTGCCGCTCTA	7786–7806	Antisense
	Sequencing primers			
	JF3S	TGAGGTCCATGCTAACAGA	5209–5228	Sense
	JF4S	TCGAGGGGGAGCCTGGAGAT	5870–5889	Sense
	JF3AS	GAGTGTCTAACTGTTTCCCAG	7220–7200	Antisense

[a] Reference strain: Gene Bank accession no. AB114136.

2.2. Cell culture

The human hepatoma cell line Huh-7 was maintained in Dulbecco's modified Eagle's medium (DMEM) supplemented with MEM non-essential amino acids (Invitrogen) 100 units/ml penicillin, 100 μg/ml streptomycin, and 10% fetal bovine serum (FBS) at 37 °C in a 5% CO_2 incubator. HCV replicon cells JFH-1/4-1 (Miyamoto et al., 2006), which are Huh-7-derived cells carrying a subgenomic replicon of JFH-1 (Kato et al., 2003) were maintained in the Huh-7 medium as above, supplemented with 1 mg/ml G418 (Nacalai Tesque, Kyoto, Japan).

2.3. Quantification of HCV RNA

Total RNA was isolated from harvested cells using Trizol (Invitrogen). Copy numbers of the viral RNA were determined by real-time RT-PCR involving single-tube reactions and performed using TaqMan EZ RT-PCR Core Reagents (PE Applied Biosystems, Foster City, CA, USA), as described previously (Aizaki et al., 2003; Takeuchi et al., 1999).

2.4. Cell viability assay

Cells were seeded at density of 5×10^4 cells/well in 24-well plates and RBV at various concentrations was added on the next day. Cultures were further incubated for 3 days at 37 °C under a humidified 5% CO_2 atmosphere. Cytotoxicity assay was performed by Cell Titer-GLO™ Luminescent Cell Viability Assay (Promega, Madison, WI, USA) according to the manufacturer's instructions. Luciferase activities were quantified with LUMAT LB 9501 (Berthold Technologies, Bad Wilbad, Germany).

2.5. Isolation and nucleotide sequencing of HCV nonstructural regions from replicon-containing cells

Total cellular RNA was isolated from replicon cells with or without RBV treatment as described above. cDNA synthesis was carried out by using Super ScriptTM III First-Strand Synthesis System for RT-PCR (Invitrogen) with primer JF1AS for NS34AB region and JF2AS for NS5AB region. Two cDNA fragments, corresponding to NS3–NS4B and NS5A–NS5B regions, were amplified by PCR using Takara EX Taq DNA polymerase (Takara BIO, Kyoto, Japan) and specific primers (Table 1; Date et al., 2004). PCR products were subcloned into pGEM-T vector (Promega) and inserts were sequenced using QIA prep® Spin Mini Prep kit (QIAGEN, Tokyo, Japan). Nucleotide sequences were analyzed with the 3100 Avant Genetic Analyzer (PE Applied Biosystems).

2.6. Plasmid constructions

pSGR-JFH1/luc, a subgenomic replicon construct with luciferase reporter derived from HCV genotype 2a JFH-1 isolate was reported previously (Miyamoto et al., 2006). Mutant replicons carrying T1134S, P1969S, V2405A, and Y2471H were created by PCR-based site-directed mutagenesis and cDNA fragments containing the above mutations were inserted into the corresponding sites of pSGR-JFH/luc. All plasmids were confirmed by sequencing the entire PCR-generated inserts. Each mutant is referred to by the original amino acid (one letter code) followed by the residue positions within the complete open reading frame of full-length JFH-1 and the substituted amino acid (one letter code).

2.7. RNA synthesis and transient replication assay

The transient replication assay method was described previously (Kato et al., 2005). Briefly, purified plasmids of pSGR-JFH1/Luc, -JFH1/Luc-T1134S, -JFH/Luc-P1969S, -JFH/Luc-V2405A and -JFH/Luc-Y2471H were linearized with XbaI and were treated with proteinase K and SDS, followed by phenol–chloroform extraction. RNA was synthesized with Ampliscribe™ T7 Transcription Kits (Epicentre BIO Technologies, Madison, WI, USA). Each transcribed RNA (5 μg) was electroporated into 2.5×10^6 of Huh7 cells pulsed at 290 mV, 975uFD with Gene pulser II apparatus (Bio-Rad Laboratories, Hercules, CA, USA). Transfected cells were resuspended in growth medium without selection antibiotics and were plated in 24-well plates at 6×10^4 cells per well. Cells were harvested at different time points post-transfection and were lysed in Passive Lysis Buffer (Promega). Luciferase activity in cells was determined using the Luciferase Assay System (Promega).

3. Results

3.1. Selection of replicon variants derived from genotype 2a with reduced susceptibility to RBV

It has been reported that RBV inhibits HCV RNA replication in Huh-7 cells bearing the viral subgenomic replicon RNAs with the EC_{50} (50% effective concentration) values of 15–225 μM (Zhou et al., 2003; Tanaka et al., 2004; Kato et al., 2005; aus dem Siepen et al., 2007). To select for RBV-associated replicon variants, cells bearing a genotype 2a HCV replicon were serially passed in the presence of 200 μM RBV as well as 1 mg/ml G418. After 20-week treatment, variant cells were then tested for RBV resistance. HCV RNA levels were determined after a 72-h incubation with various concentrations of RBV in the absence of G418, and about 5-fold-reduced susceptibility to RBV was observed in the variant replicon

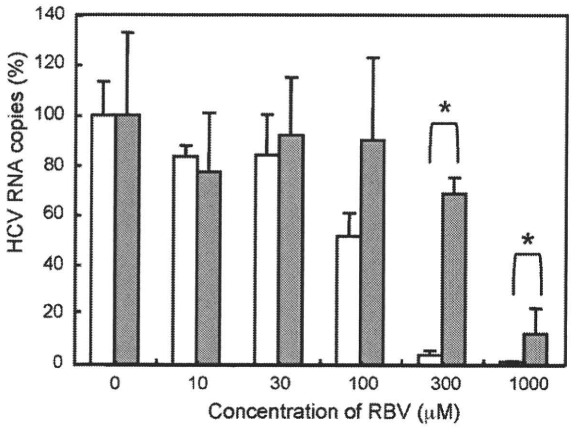

Fig. 1. Inhibitory effect of RBV on HCV RNA levels in genotype 2a replicon cells after long-term treatments with RBV. The replicon cells were serially passaged in 0 or 200 μM RBV for 20 weeks. The cells were then split and incubated with fresh RBV at various concentrations in the absence of G418 for 3 days, followed by the determination of HCV RNA. Clear bars, passage in the absence of RBV: gray bars, passage in the presence of RBV. HCV RNA copies per microgram of total RNA were normalized as percentages of those of untreated (RBV 0 μM). Each data point is presented as the mean of three independent determinations with standard deviation. *$p < 0.05$.

cells; the EC_{50} values for the variant and wild-type replicon cells were 470 and 102 μM, respectively (Fig. 1). Comparable cytotoxic effects of RBV were observed against wild-type and variant replicon cells, with the CC_{50} (50% cytotoxicity concentration) values of 151 and 156 μM, respectively (data not shown).

3.2. Mapping RBV resistance to cell line or replicon RNA

To test whether reduced susceptibility to RBV in the variant cells observed as above was due to the appearance of mutations within the viral RNA or was cell-derived, total RNAs from the variant and wild-type replicon cells were extracted and used for retransfection of naïve Huh7 cells. Retransfected cells resistant to G418 were established after 4 weeks of cultures in the presence of 1 mg/ml G418 and were assessed for HCV RNA replication sensitivity to RBV (Fig. 2A). HCV RNA levels in the cells obtained from the wild-type replicon were inhibited by 56, 89 and 97% with 100, 300 and 1000 μM RBV, respectively. By contrast, the culture retransfected with RNA derived from the variant replicon cells exhibited inhibition levels of 13, 29 and 89% with the corresponding concentrations of RBV. EC_{50} values were calculated to be 93 and 449 μM, respectively. We confirmed the presence of replicon mutations, as described below, in the cells retransfected with RNA derived from the variant replicon cells.

In order to explore the possibility for cell-derived resistance, both wild-type and variant replicon cells were cured of viral RNAs by IFN treatment; cells were passaged with media containing 100 IU/mL IFN-α in the absence of G418 for 2 months. To compare RBV sensitivity, cured cells were transiently transfected with the wild-type JFH-1 subgenomic replicon RNA and were treated with various concentrations of RBV for 72 h. Similar anti-HCV effects of RBV were observed in the cured cells derived from wild-type and variant replicons, with the EC_{50} values of 147 and 118 μM, respectively (Fig. 2B). Thus, the results suggest that the RBV resistance observed may arise by mutations in the replicon rather than by changes in the cells.

3.3. HCV mutations in replicon variant with reduced susceptibility to RBV

It has been reported that mutations in RNA virus genomes responsible for RBV resistance are mostly present in the coding region for the viral RNA-dependent RNA polymerase (RdRp). On the other hand, it is known that RBV works as an RNA mutagen to generate rapidly mutating viral RNA and that NS5B RdRp and other nonstructural proteins in HCV are involved in the viral replication complex, playing key roles in genome replication. Therefore, we sequenced the coding regions for NS3 through NS5B proteins of the replicon molecules in order to determine whether mutations associated with RBV resistance were generated. As shown in Table 2, there were numerically more synonymous and non-synonymous mutations in the RBV-resistant variant replicon cells (RBV treatment) when compared with untreated replicative conditions (No-treatment) across most regions examined. Mutation frequencies of NS3, NS4B and NS5A regions of RBV treatment were significantly higher than those of No-treatment. The total number of synonymous mutations in the RBV-resistant variant replicon cells was 3 times higher than that under untreated replicative conditions, and the number of non-synonymous mutations in the RBV-resistant variant replicon cells was 1.5 times higher than that under untreated replicative conditions. The number of both synonymous and non-synonymous mutations (NS3, NS4B, NS5A and NS5B regions) in the RBV-resistant replicon cells was greater than that in the control cells. We also found a large number of transition

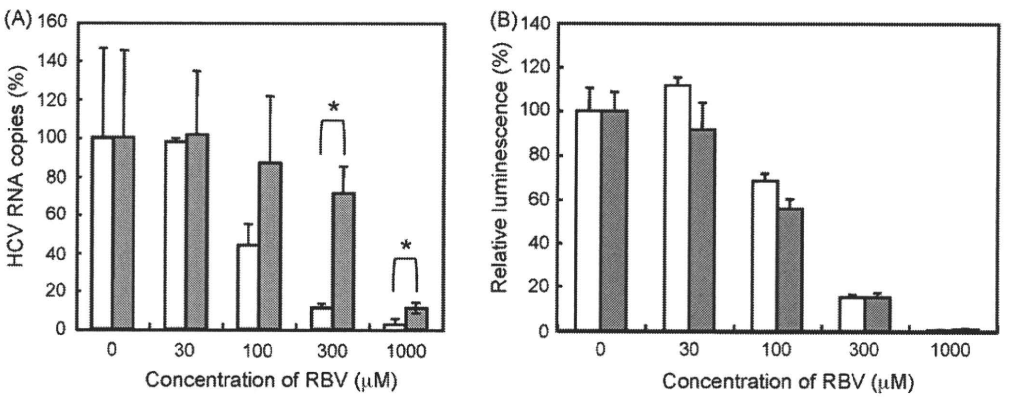

Fig. 2. Testing for replicon-derived resistance (A) or for cell-derived resistance (B). (A) Total RNA from RBV-resistant- or wild-type replicon cells was transfected into naïve Huh7 cells. After selection in 1 mg/ml G418 for 4 weeks, re-established replicon cells, wild-type derived (clear bars) and RBV resistance derived (gray bars), were treated with increasing concentrations of RBV in the absence of G418 for 3 days. HCV RNA copies per microgram total RNA were assessed and the levels from wild-type cells without RBV treatment were set at 100%. Data are indicated as means with standard deviations. *$p < 0.05$. (B) RBV-resistant- or wild-type replicon cells were cured by passage in IFN-α in the absence of G418. Cured cells were transiently transfected with the replicon RNA derived from pSGR-JFH1/luc. Transient replication assay of transfectants derived from wild-type (clear bars) and RBV resistance (gray bars) was performed after treatment with various concentrations of RBV for 72 h. The values for wild-type-derived cells without RBV treatment were set at 100%. Data are indicated as means with standard deviations.

Table 2
Mutation frequencies in HCV NS regions after 20-weeks culture with or without RBV treatment.

Region	nt length	No-treatment			RBV treatment		
		No. of non-synonymous mutations[a]	No. of synonymous mutations[a]	Mutation frequency (10^{-3})	No. of non-synonymous mutations[a]	No. of synonymous mutations[a]	Mutation frequency (10^{-3})
NS3	1893	1.7 ± 2.1	2.3 ± 1.5	2.1	4.7 ± 2.4	6.5 ± 2.5	5.9[b]
NS4A	165	1.0 ± 1.0	0.3 ± 0.6	8.1	0.3 ± 0.5	0.5 ± 0.9	4.4
NS4B	780	1.3 ± 1.2	0.3 ± 0.6	2.1	2.3 ± 1.5	2.5 ± 1.2	4.7[c]
NS5A	1380	4.0 ± 1.2	2.0 ± 1.2	4.3	5.9 ± 1.2	6.2 ± 2.4	12.2[c]
NS5B	1773	4.5 ± 1.5	2.3 ± 1.5	3.8	4.8 ± 1.8	4.2 ± 1.1	9.0
NS3–NS5B	5991	12.5 ± 2.7	7.3 ± 2.7	-	17.8 ± 4.5	20.1 ± 4.6	-

[a] Values are means ± standard deviations.
[b] $p < 0.05$ relative to No-treatment by the unpaired t-test.
[c] $p < 0.01$ relative to No-treatment by the unpaired t-test.

mutations in RBV-resistant cells, particularly G-to-A and C-to-U transitions, as expected from previous studies. Although mutations were distributed throughout nonstructural regions, four major amino acid substitutions; T1134S in the NS3 region, P1969S in NS4B, V2405A in NS5A, and Y2471H in NS5B, not seen in wild-type cells were observed in most of the subclones among RBV-resistant replicon cells. T1134S, P1969S, V2405A, and Y2471H were present, respectively, in 7 of 11, 6 of 11, 8 of 13, and 7 of 13 PCR subclones sequenced.

3.4. Effects of T1134S, P1969S, V2405A, and Y2471H on RBV susceptibility

To test the possibility that any of the four mutations as identified confer resistance to RBV, we introduced these mutations individually into the JFH-1 subgenomic replicon containing a luciferase reporter gene. Cells transfected with mutant- or wild-type replicon RNA grown in the presence of various concentrations of RBV for 2 or 3 days. As demonstrated in Fig. 3A, the replication levels of all four mutant replicons (SGR-JFH1/Luc-T1134S, -P1969S, -V2405A, and -Y2471H) in the presence of 125 or 500 μM RBV were higher than those of the wild-type replicon. In particular, the Y2471H mutant significantly reduced susceptibility to RBV; replication levels of SGR-JFH1/Luc-Y2471H were 3–5-fold higher when compared to those of wild-type under the present assay conditions.

The relative replication activity of these mutant replicons was further determined in 3-day replication assay without drug treatment (Fig. 3B). All mutant replicons exhibited reduced efficiency relative to the wild-type replicon. Levels of the Y2471H-mutated replicon were approximately 30% of those of the wild-type, thus suggesting that replicon mutants with reduced sensitivity to RBV are associated with decreased replication fitness.

4. Discussion

It is generally accepted that, during chemotherapy against viral infection, high rates of viral replication and high frequencies of mutation lead to generation of drug-resistant mutants. Although several potential mechanisms for the inhibition of HCV replication by RBV have been proposed, the molecular mechanisms involved in the generation of RBV-resistant HCV remain poorly understood.

This study found that long-term treatment of HCV JFH-1-derived replicon cells with RBV leads to selection of preferential mutations in NS3 (T1134S), NS4B (P1969S), NS5A (V2405A) and NS5B (Y2471H) genes. Each mutation only required a single nucleotide change, and P1969S, V2405A and Y2471H are transition mutations, which are known to be commonly caused by incorporated RBV. Site-directed mutagenesis of these mutations into the replicon demonstrated that Y2471H plays a role in reduced susceptibility to RBV.

Crystal structure information revealed that HCV RdRp is organized into an arrangement with palm, fingers, and thumb subdomains (Lesburg et al., 1999). Residue 2471 (the 33rd position of NS5B) is present in the N-terminal loop region that bridges the fingers. Although this site is apparently distant from the active site of the polymerase in the palm region, it has been reported

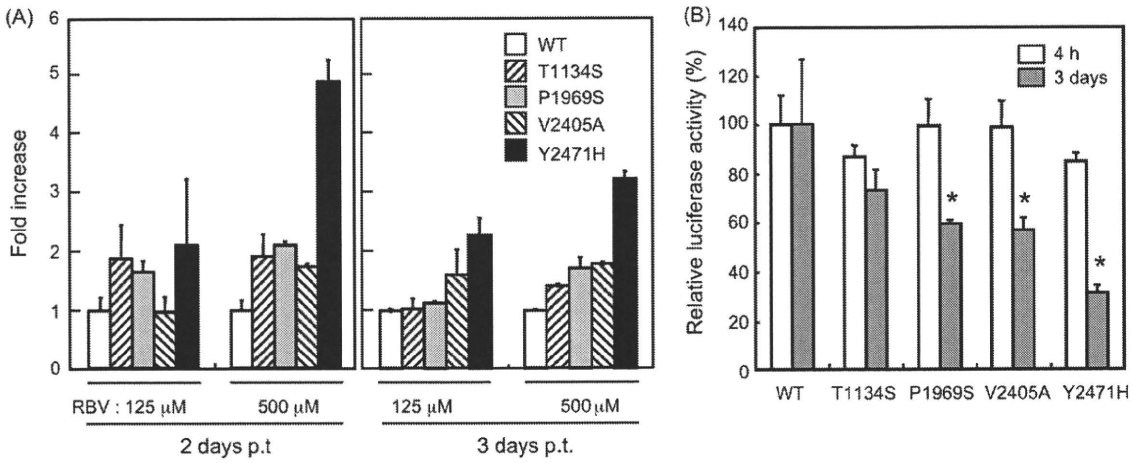

Fig. 3. Impact of major mutations in NS3–NS5B regions on RBV susceptibility (A) and replication capacity (B). Mutated replicons carrying single residue substitutions (T1134S, P1969S, V2405A, and Y2471H) were constructed and used for transient replication assay. Cells were transfected with either wild-type (WT) or with mutant replicon RNA in the absence or presence (125, 500 μM) of RBV. Luciferase activity was assessed at 4 h, 2 days and 3 days post-transfection (p.t.). (A) Luciferase activities of WT were set at 1, and the fold increases in the activities of mutants were plotted. (B) Luciferase activities in the absence of RBV at 4 h and 3 days post-transfection were shown. The activities of mutants were normalized as percentages of the WT activities. Data from triplicate samples were averaged and indicated with standard deviations. *$p < 0.05$ against WT.

that small molecules, such as benzimidazole compounds, are able to specifically bind the fingers-thumb interface and inhibit polymerase activity (Herlihy et al., 2008), thus suggesting that amino acid substitutions in the loop region may affect RNA polymerization. The involvement of tyrosine residue at position 415 of HCV NS5B in RBV resistance has been previously described for patients with genotype 1a infection and for the genotype 1b replicon (Young et al., 2003). Although the mechanism for resistance remains elusive, it has been hypothesized that RBV interacts with RdRp around this residue, which is located in the thumb subdomain, thus affecting RNA polymerization (Young et al., 2003).

Based on analysis of available sequences from Genbank, tyrosine at the 33rd residue of NS5B is conserved in all isolates of genotype 2a, but not in other genotypes. In genotype 1a and 1b isolates, 96% contain histidine and only a small population contains tyrosine or asparagine at the site. All the isolates of genotypes 3, 4, 5 and 6 contain histidine, whereas phenylalanine is conserved for genotype 2b. It should be noted that V2405 and P1969 are also completely conserved for genotype 2a but not for other genotypes. Therefore, it is likely that the identified HCV variants with reduced susceptibility to RBV are genotype-specific. It will be of interest to determine whether HCV genotype 2a is intrinsically more sensitive to RBV when compared with other genotypes.

At present, at least 4 mechanisms of action of RBV are proposed (Lau et al., 2002). They include (1) direct inhibition of the HCV replication machinery, (2) as an RNA mutagen that drives a rapidly mutating RNA virus over the threshold to "error catastrophe", (3) inhibition of the host enzyme inosine monophosphate dehydrogenase (IMPDH), and (4) enhancement of host T-cell-mediated immunity against viral infection. In addition to the direct inhibition, it is also possible that other mechanisms such as error-prone and IMPDH-inhibition are involved in HCV escape from RBV treatment. Further investigation of the interaction of HCV variants with the viral and cellular factors involved in viral resistance may improve understanding of the mechanism(s) of RBV resistance.

In conclusion, RBV encountered resistance from the HCV genotype 2a replicon largely mediated by mutations in the N-terminal region of NS5B. Although whether these mutagenic effects are also demonstrable in IFN-RBV combination therapy will require further studies, the mutations identified in this study represent the first drug-resistant variants belonging to HCV genotype 2a. The drug resistance patterns found in this study may be of benefit in prediction in vivo resistance profiles and the development of next-generation nucleoside analogues as anti-HCV drugs.

Acknowledgments

We thank M. Matsuda, S. Yoshizaki, M. Ikeda, T. Shimoji, M. Kaga and M. Sasaki for their technical assistance. This work was supported by a grant-in-aid for Scientific Research from the Japan Society for the Promotion of Science, from the Ministry of Health, Labour and Welfare of Japan and from the Ministry of Education, Culture, Sports, Science and Technology, and by Research on Health Sciences focusing on Drug Innovation from the Japan Health Sciences Foundation, Japan and by the Program for Promotion of Fundamental Studies in Health Sciences of the National Institute of Biomedical Innovation of Japan. S.S.H. is the recipient of a Research Resident Fellowship from Viral Hepatitis Research Foundation of Japan.

References

Aizaki, H., Nagamori, S., Matsuda, M., Kawakami, H., Hashimoto, O., Ishiko, H., Kawada, M., Matsuura, T., Hasumura, S., Matsuura, Y., Suzuki, T., Miyamura, T., 2003. Production and release of infectious hepatitis C Virus for human liver cell cultures in the three-dimensional radial-flow bioreactor. Virology 314, 16–25.

aus dem Siepen, M., Oniangue-Ndza, C., Wiese, M., Ross, S., Roggendorf, M., Viazov, S., 2007. Interferon-alpha and ribavirin resistance of Huh7 cells transfected with HCV subgenomic replicon. Virus Res. 125, 109–113.

Date, T., Kato, T., Miyamoto, M., Zhao, Z., Yasui, K., Mizokami, M., Wakita, T., 2004. Genotype 2a hepatitis C virus subgenomic replicon can replicate in HepG2 and IMY-N9 cells. J. Biol. Chem. 279, 22371–22376.

Domingo, E., 1996. Biological significance of viral quasispecies. Viral Hep. Rev. 2, 247–261.

Farci, P., Purcell, R.H., 2000. Clinical significance of hepatitis C virus genotypes and quasispecies. Semin. Liver Dis. 20, 103–126.

Forns, X., Purcell, R.H., Bukh, J., 1999. Quasispecies in viral persistence and pathogenesis of hepatitis C virus. Trends Microbiol. 7, 402–410.

Fried, T.R., Bradley, E.H., Towle, V.R., Allore, H., 2002. Understanding the treatment preferences of seriously ill patients. N. Engl. J. Med. 346, 1061–1066.

Herlihy, K.J., Graham, J.P., Kumpf, R., Patick, A.K., Duggal, R., Shi, S.T., 2008. Development of intragenotypic chimeric replicons to determine the broad-spectrum antiviral activities of hepatitis C virus polymerase inhibitors. Antimicrob. Agents Chemother. 52, 3523–3531.

Kato, T., Date, T., Miyamoto, M., Furusaka, A., Tokushige, K., Mizokami, M., Wakita, T., 2003. Efficient replication of the genotype 2a hepatitis C virus subgenomic replicon. Gastroenterology 125, 1808–1817.

Kato, T., Date, T., Miyamoto, M., Sugiyama, M., Tanaka, Y., Orito, E., Ohno, T., Sugihara, K., Hasegawa, I., Fujiwara, K., Ito, K., Ozasa, A., Mizokami, M., Wakita, T., 2005. Detection of anti-hepatitis C virus effects of interferon and ribavirin by a sensitive replicon system. J. Clin. Microbiol. 43, 5679–5684.

Lau, J.Y., Tam, R.C., Liang, T.J., Hong, Z., 2002. Mechanism of action of ribavirin in the combination treatment of chronic HCV infection. Hepatology 35, 1002–1009.

Lesburg, C.A., Cable, M.B., Ferrari, E., Hong, Z., Mannarino, A.F., Weber, P.C., 1999. Crystal structure of the RNA-dependent RNA polymerase from hepatitis C virus reveals a fully encircled active site. Nat. Struct. Biol. 6, 937–943.

Manns, M.P., McHutchison, J.G., Gordon, S.C., Rustgi, V.K., Shiffman, M., Reindollar, R., Goodman, Z.D., Koury, K., Ling, M., Albrecht, J.K., 2001. Peginterferon alfa-2b plus ribavirin compared with interferon alfa-2b plus ribavirin for initial treatment of chronic hepatitis C: a randomised trial. Lancet 358, 958–965.

Martell, M., Esteban, J.I., Quer, J., Genesca, J., Weiner, A., Esteban, R., Guardia, J., Gomez, J., 1992. Hepatitis C virus (HCV) circulates as a population of different but closely related genomes: quasispecies nature of HCV genome distribution. J. Virol. 66, 3225–3229.

Miyamoto, M., Kato, T., Date, T., Mizokami, M., Wakita, T., 2006. Comparison between subgenomic replicons of hepatitis C virus genotypes 2a (JFH-1) and 1b (con1 NK5.1). Intervirology 49, 37–43.

Pfeiffer, J.K., Kirkegaard, K., 2005. RBV resistance in hepatitis C virus replication containing cells conferred by changes in the cell line or mutations in the replicon RNA. J. Virol. 79, 2346–2355.

Simmonds, P., Gallin, J.I., Farrei, A.S., 2000. Hepatitis C virus genotypes. Biomed. Res. Rep. 2, 53–70.

Takeuchi, T., Katsume, A., Tanaka, T., Abe, A., Inoue, K., Tsukiyama Kohara, K., Kawaguchi, R., Tanaka, S., Kohara, M., 1999. Real-time detection system for quantification of Hepatitis C virus genome. Gastroenterology 116, 636–642.

Tanaka, Y., Sakamoto, N., Enomoto, N., Kurosaki, M., Ueda, E., Maekawa, S., Yamashiro, T., Nakagawa, M., Chen, C.-H., Kanazawa, N., Kakinuma, S., 2004. Synergistic inhibition of intracellular hepatitis C virus replication by combination of ribavirin and interferon-alpha. J. Infect. Dis. 189, 1129–1139.

World Health Organization (WHO), 2000. Hepatitis C: global prevalence (update). Weekly Epidemiological Record, WHO 75, 18–19.

Young, K.C., Lindsay, K.L., Lee, K.J., Liu, W.C., He, J.W., Milstein, S.L., Lai, M.M., 2003. Identification of a ribavirin-resistant NS5B mutation of hepatitis C virus during ribavirin monotherapy. Hepatology 38, 869–878.

Zhou, S., Liu, R., Baroudy, B.M., Malcolm, B.A., Reyes, G.R., 2003. The effect of ribavirin and IMPDH inhibitors on hepatitis C virus subgenomic replicon RNA. Virology 310, 333–342.

JOURNAL OF VIROLOGY, Nov. 2010, p. 11761–11770 Vol. 84, No. 22
0022-538X/10/$12.00 doi:10.1128/JVI.00638-10

Sphingomyelin Activates Hepatitis C Virus RNA Polymerase in a Genotype-Specific Manner▽†

Leiyun Weng,[1] Yuichi Hirata,[2] Masaaki Arai,[3] Michinori Kohara,[2] Takaji Wakita,[4] Koichi Watashi,[4,5] Kunitada Shimotohno,[5,6] Ying He,[7] Jin Zhong,[7] and Tetsuya Toyoda[1]*

Units of Viral Genome Regulation[1] and Viral Hepatitis,[7] Institut Pasteur of Shanghai, Key Laboratory of Molecular Virology and Immunology, Chinese Academy of Sciences, 411 Hefei Road, 200025 Shanghai, People's Republic of China; Department of Microbiology and Cell Biology, Tokyo Metropolitan Institute of Medical Biology, 3-18-22 Honkomagome, Bunkyo-Ku, Tokyo 113-8613, Japan[2]; Pharmacology Laboratory, Pharmacology Department V, Mitsubishi Tanabe Pharma Corporation, 1000 Kamoshida-cho, Aoba-ku, Yokohama 227-0033, Japan[3]; Department of Virology II, National Institute of Health, 1-23-1 Toyama, Shinjuku, Tokyo 132-8640, Japan[4]; Laboratory of Human Tumor Viruses, Department of Viral Oncology, Institute for Virus Research, Kyoto University, Kyoto 606-8507, Japan[5]; and Chiba Institute of Technology, 2-17-1 Tsudamuna, Narashino, Chiba 275-0016, Japan[6]

Received 25 March 2010/Accepted 27 August 2010

Hepatitis C virus (HCV) replication and infection depend on the lipid components of the cell, and replication is inhibited by inhibitors of sphingomyelin biosynthesis. We found that sphingomyelin bound to and activated genotype 1b RNA-dependent RNA polymerase (RdRp) by enhancing its template binding activity. Sphingomyelin also bound to 1a and JFH1 (genotype 2a) RdRps but did not activate them. Sphingomyelin did not bind to or activate J6CF (2a) RdRp. The sphingomyelin binding domain (SBD) of HCV RdRp was mapped to the helix-turn-helix structure (residues 231 to 260), which was essential for sphingomyelin binding and activation. Helix structures (residues 231 to 241 and 247 to 260) are important for RdRp activation, and 238S and 248E are important for maintaining the helix structures for template binding and RdRp activation by sphingomyelin. 241Q in helix 1 and the negatively charged 244D at the apex of the turn are important for sphingomyelin binding. Both amino acids are on the surface of the RdRp molecule. The polarity of the phosphocholine of sphingomyelin is important for HCV RdRp activation. However, phosphocholine did not activate RdRp. Twenty sphingomyelin molecules activated one RdRp molecule. The biochemical effect of sphingomyelin on HCV RdRp activity was virologically confirmed by the HCV replicon system. We also found that the SBD was the lipid raft membrane localization domain of HCV NS5B because JFH1 (2a) replicon cells harboring NS5B with the mutation A242C/S244D moved to the lipid raft while the wild type did not localize there. This agreed with the myriocin sensitivity of the mutant replicon. This sphingomyelin interaction is a target for HCV infection because most HCV RdRps have 241Q.

Hepatitis C virus (HCV) has a positive-stranded RNA genome and belongs to the family *Flaviviridae* (21). HCV chronically infects more than 130 million people worldwide (34), and HCV infection often induces liver cirrhosis and hepatocellular carcinoma (19, 28). To date, pegylated interferon (PEG-IFN) and ribavirin are the standard treatments for HCV infection. However, many patients cannot tolerate their serious side effects. Therefore, the development of new and safer therapeutic methods with better efficacy is urgently needed.

Lipids play important roles in HCV infection and replication. For example, the HCV core associates with lipid droplets and recruits nonstructural proteins and replication complexes to lipid droplet-associated membranes which are involved in the production of infectious virus particles (24). HCV RNA replication depends on viral protein association with raft membranes (2, 30). The association of cholesterol and sphingolipid with HCV particles is also important for virion maturation and infectivity (3). The inhibitors of the sphingolipid biosynthetic pathway, ISP-1 and HPA-12, which specifically inhibit serine palmitoyltransferase (SPT) (23) and ceramide trafficking from the endoplasmic reticulum (ER) to the Golgi apparatus (37), suppress HCV virus production in cell culture but not viral RNA replication by the JFH1 replicon (3). Other serine SPT inhibitors (myriocin and NA255) inhibit genotype 1b replication (4, 29, 33). Very-low-density lipoprotein (VLDL) also interacts with the HCV virion (15).

Sakamoto et al. reported that sphingomyelin bound to HCV RNA-dependent polymerase (RdRp) at the sphingomyelin binding domain (SBD; amino acids 230 to 263 of RdRp) to recruit HCV RdRp on the lipid rafts, where the HCV complex assembles, and that NA255 suppressed HCV replication by releasing HCV RdRp from the lipid rafts (29). In the present study, we analyzed the effect of sphingomyelin on HCV RdRp activity *in vitro* and found that sphingomyelin activated HCV RdRp activity in a genotype-specific manner. We also determined the sphingomyelin activation domain and the activation mechanism. Finally, we confirmed our biochemical data by a HCV replicon system.

MATERIALS AND METHODS

HCV RNA polymerase. A C-terminal 21-amino-acid deletion was made to the HCV RdRps of strains HCR6 (genotype 1b) (36), NN (1b) (35), Con1 (1b) (5), JFH1 (2a) (36), J6CF (2a) (25), H77 (1a) (7), and RMT (1a), and the mutants

* Corresponding author. Mailing address: Unit of Viral Genome Regulation, Institut Pasteur of Shanghai, Chinese Academy of Sciences, 411 Hefei Road, 200025 Shanghai, People's Republic of China. Phone and fax: 86 21 6385 1621. E-mail: ttoyoda@amber.plala.or.jp.

† Supplemental material for this article may be found at http://jvi.asm.org.

▽ Published ahead of print on 15 September 2010.

were purified from bacteria as described previously (36). HCR6 (1b) RdRp with the mutation L245A [RdRp(L245A)] or I253A [RdRp(I253A)] or the double mutation L245A and I253A [RdRp(L245A/I253A)]; JFH1 (2a) RdRp with the mutation(s) A242C/S244D, A242, S244D, or T251Q; J6CF (2a) RdRp with the mutation(s) R241Q, S244D, or R241Q/S244D; and H77 (1a) RdRp(A238S/Q248E) were introduced using an *in vitro* mutagenesis kit (Stratagene) and the oligonucleotides listed in Table S1 in the supplemental material. HCR6 (1b) His_6-tagged RdRp(L245A/I253A) was removed from pET21b/KM (36) and cloned into the BamHI/XhoI site of pGEX-6P-3 (GE), resulting in pGEXHCVHCR6RdRp(L245A/I253A).

***In vitro* HCV transcription.** *In vitro* HCV transcription was performed as described previously (36). Briefly, following 30 min of preincubation without ATP, CTP, or UTP, 100 nM HCV RdRp was incubated in 50 mM Tris-HCl (pH 8.0), 200 mM monopotassium glutamate, 3.5 mM $MnCl_2$, 1 mM dithiothreitol (DTT), 0.5 mM GTP, 50 μM ATP, 50 μM CTP, 5 μM [α-^{32}P]UTP, 200 nM RNA template (SL12-1S), 100 U/ml human placental RNase inhibitor, and the lipid (amount indicated below) at 29°C for 90 min. ^{32}P-labeled RNA products were subjected to 6% polyacrylamide gel electrophoresis (PAGE) containing 8 M urea. The resulting autoradiograph was analyzed with a Typhoon Trio plus image analyzer (GE).

RNA filter binding assay. An RNA filter binding assay was performed as described previously (36). Briefly, 100 nM HCV RdRp and 100 nM ^{32}P-labeled RNA template (SL12-1S) were incubated with or without 0.01 mg/ml egg yolk sphingomyelin in 25 μl of 50 mM Tris-HCl (pH 7.5), 200 mM monopotassium glutamate, 3.5 mM $MnCl_2$, and 1 mM DTT at 29°C for 30 min. After incubation, the solutions were diluted with 0.5 ml of TE (50 mM Tris-HCl [pH 7.5], 1 mM EDTA) buffer and filtered through nitrocellulose membranes (0.45-μm pore size; Millipore). The filter was washed five times with TE buffer, and the bound radioisotope was analyzed by Typhoon Trio plus after being dried.

Enzyme-linked immunosorbent assay (ELISA). Ninety-six-well microtiter plates (Corning) were coated with 250 ng of egg yolk sphingomyelin in ethanol by evaporation at room temperature. After the wells were blocked with phosphate-buffered saline (PBS) and 3% bovine serum albumin (BSA), they were incubated with 1 pmol of the HCV RdRp of HCR6 (1b) wild type (wt) or L245A, I253A, or L245A/I253A mutant; NN (1b); H77 (1a); RMT (1a); J6CF (2a); or JFH1 (2a) wt or A242C/S244D, A242, S244D, or T251Q mutant in Tris-buffered saline (50 mM Tris-HCl [pH 7.5] and 150 mM NaCl) for 1.5 h at room temperature. After being blocked with 3% BSA, the bound HCV RdRp was detected by adding rabbit anti-HCV RdRp serum (1:5,000) (see Fig. S1 in the supplemental material) (17) before incubation with a horseradish peroxidase (HRP)-conjugated anti-rabbit IgG antibody (1:5,000; Southern Biotech). The optical density at 450 nm (OD_{450}) was measured with a Spectra Max 190 spectrophotometer (Molecular Devices) using a TMB (3,3′,5,5′-tetramethylbenzidine) Liquid Substrate System (Sigma).

HCV subgenomic replicon. A D244S mutation was introduced into the HCV strain NN (1b) subgenomic replicon pLMH14 (35), resulting in pLMH(NN)5B(D244S) [where 5B(D244S) is the NS5B protein with the mutation D244S]. The A242C/S244D mutation was introduced into the HCV JFH1 (2a) replicon, pSGR-JFH1/luc (25), resulting in pSGR-JFH1/luc5B(A242C/S244D). The HpaI and XbaI fragment of pSGR-JFH1 (18) was replaced with that of pSGR-JFH1/luc5B(A242C/S244D), resulting in pSGR-JFH15B(A242C/S244D). The A238S/Q248E mutation was introduced into HCV H77 (1a) replicon pHCVrep13(S2204I)/Neo (7) after the neomycin gene was replaced by the firefly luciferase gene [pH77(I)/luc] by insertion of AflII and AscI sites (see Table S1 in the supplemental material), resulting in pH77(I)/luc5B(A238S/Q248E). Subgenomic replicon RNA was transcribed *in vitro* by T7 RNA polymerase using MegaScript (Ambion) after the replicon plasmids were linearized by XbaI (strain NN and JFH1 replicons) or HpaI (strain H77 replicon). Subgenomic replicon RNA was stored at −80°C after being purified by phenol-chloroform extraction and ethanol precipitation.

Replicon assay with myriocin. Huh7.5.1 cells were kindly provided by F. Chisari and were maintained in Dulbecco's modified Eagle's medium (DMEM; Gibco) with 10% fetal bovine serum (FBS; Gibco) (38). HCV replicon RNA (10 μg) was transfected into 4×10^6 Huh7.5.1 cells (1×10^7/ml) in OptiMEM I (Gibco) by electroporation (GenePulser Xcell; Bio-Rad) at 270 V, 100 Ω, and 950 μF. After transfection, the cells were plated in 12-well plates incubated in DMEM–10% FBS. At 6 h after transfection, cells were treated with 0, 5, and 50 nM myriocin. At 4, 54, and 78 h after transfection (48 and 72 h after myriocin treatment), the cells were harvested, and luciferase activity was measured using a Dual-Glo luciferase assay kit and a GloMax 96 Microplate Luminometer (Promega). Luciferase activity was normalized against the activity at 4 h after transfection (26).

HCV JFH1 wt and NS5B(A242C/S244D) replicon cells. Huh7/scr cells were kindly provided by F. Chisari of the Scripps Research Institute and were maintained in Dulbecco's modified Eagle's medium (Gibco) with 10% fetal bovine serum (Gibco). RNA (10 μg each) from SGR-JFH1 and SGR-JFH1 with the mutations A242C/S244D in NS5B [NS5B(A242C/S244D) was transfected into 4×10^6 Huh7/scr cells (1×10^7/ml) in OptiMEM I (GIBCO) by electroporation (GenePulser Xcell; Bio-Rad) at 270 V, 100 Ω, and 950 μF. After transfection, the cells were plated in 10-cm dishes and incubated in DMEM–10% FBS with 1.0 and 0.5 mg/ml G418 (Gibco). JFH1 wt and NS5B(A242C/S244D) replicon cells were maintained in DMEM–10% FBS and 0.5 mg/ml G418.

Membrane floating assay. JFH1 wt and NS5B(A242C/S244D) replicon cells were suspended in two packed cell volumes of hypotonic buffer (10 mM HEPES-NaOH [pH 7.6], 10 mM KCl, 1.5 mM $MgCl_2$, 2 mM DTT, and 1 tablet/25 ml of EDTA-free protease inhibitor cocktail tablets [Roche]) and disrupted by 30 strokes of homogenization in a Dounce homogenizer using a tight-fitting pestle at 4°C. After nuclei were removed by centrifugation at 2,000 rpm for 10 min at 4°C, the supernatant (postnuclear supernatant [PNS]) was treated with 1% Triton X-100 in TNE buffer (25 mM Tris-HCl [pH 7.6] 150 mM NaCl, 1 mM EDTA) for 30 min on ice. The lysates were supplemented with 40% sucrose and centrifuged at 38,000 rpm in a Beckman SW41 Ti rotor (Beckman Coulter) overlaid with 30% and 10% sucrose in TNE buffer at 4°C for 14 h.

Western blotting. Western blotting using anti-HCV RdRp (17), rabbit anti-NS3 (32), anti-NS5A (16) and anti-caveolin-2 was performed as previously published (17).

Reagent. Egg yolk sphingomyelin, cholesterol phosphocholine, myriocin, and rabbit anti-caveolin-2 antibodies were purchased from Sigma. Hexanoyl sphingomyelin, C_6-ceramide, C_8-β-D-glucosyl ceramide, and C_8-β-D-lactosyl ceramide were purchased from Avanti Polar Lipids. [α-^{32}P]UTP was purchased from New England Nuclear.

Statistical analysis. Significant differences were evaluated using *P* values calculated from a Student's *t* test.

Nucleotide sequence accession number. The sequence of HCV RMT has been deposited in the GenBank under accession number AB520610.

RESULTS

Sphingomyelin activation of HCV RNA polymerases of various genotypes. There are several sequence variations in the sphingomyelin binding domain (SBD; amino acids 231 to 260 of HCV RdRp) among HCV genotypes (see Fig. 7A). In order to compare the RdRps of different genotypes of HCV, we purified RdRp from genotypes 1b (strains HCR6, NN, and Con1), 1a (H77 and MRT), and 2a (JFH1 and J6CF) (see Fig. S2 in the supplemental material). First, the effect of ethanol on HCV HCR6 (1b) RdRp transcription was examined because lipids were suspended in ethanol before they were added to the HCV transcription reaction mixture. We found that 2% ethanol did not inhibit HCV transcription (see Fig. S3 in the supplemental material); therefore, all subsequent experiments were performed using less than 2% ethanol.

The kinetics of sphingomyelin activation were analyzed using egg yolk sphingomyelin for HCR6 (1b) RdRp wt (Fig. 1A) and subtype 2a (JFH1 and J6CF) RdRps (Fig. 1B), and *N*-hexanoyl-D-*erythro*-sphingosylphosphorylcholine (hexanoyl sphingomyelin) was used for HCR6 (1b) RdRp wt (Fig. 1C) and subtype 1a (H77 and RMT) RdRps (Fig. 1D). The egg yolk sphingomyelin activation curve of HCR6 (1b) RdRp wt at low concentrations (<0.01 mg/ml) was sigmoid. The transcription activity of HCR6 (1b) RdRp wt increased in a dose-dependent manner. It was activated 11-fold at 0.01 mg/ml and then plateaued (14-fold activation) at 0.1 mg/ml. However, JFH1 (2a) and J6CF (2a) RdRps were activated 2.5-fold and 2.2-fold, respectively, at 0.01 mg/ml sphingomyelin, at which point they plateaued.

Egg yolk sphingomyelin is a mixture. In order to obtain the optimal molar ratio for sphingomyelin activation of HCR6 (1b)

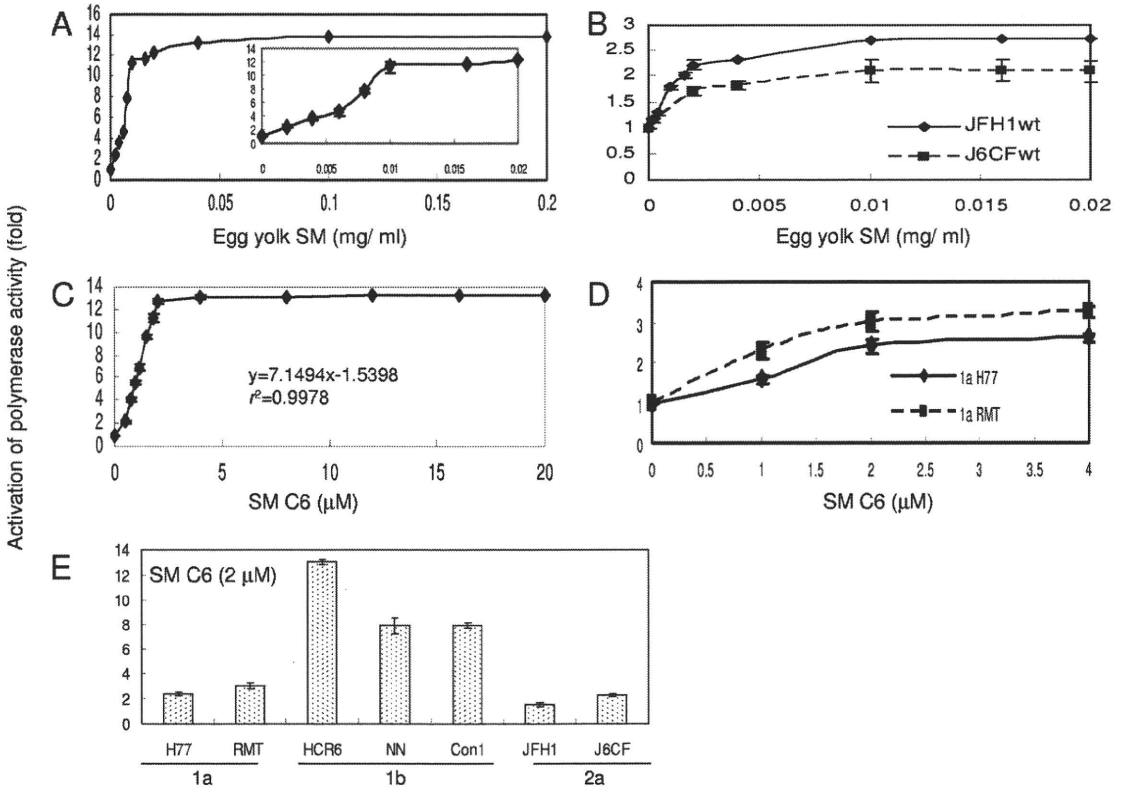

FIG. 1. Sphingomyelin activation of HCV RNA polymerases. (A) Activation kinetics of HCV HCR6 (1b) RdRp wt by egg yolk sphingomyelin (SM). The inset shows activation produced by 0 to 0.02 mg/ml egg yolk sphingomyelin. Activation kinetics of HCV 2a (JFH1 and J6CF) RdRps by egg yolk sphingomyelin (B) and of HCV HCR6 (1b) RdRp wt by hexanoyl sphingomyelin (SM C6) (C). In panel C, the first order of the graph was fitted by linear regression; the calculated equation is indicated in the graph. (D) Activation kinetics of HCV 1a (H77 and RMT) RdRps by hexanoyl sphingomyelin. (E) Activation effect of hexanoyl sphingomyelin on HCV RdRp of various genotypes. HCV RdRp (100 nM) was incubated with or without 2 μM SM C6. The names of the RdRps are indicated below the graph. Mean ± standard deviation of the activation ratio was calculated from three independent experiments.

RdRp wt, its activation kinetics were calculated using hexanoyl sphingomyelin (Fig. 1C, SM C6). The equation for the first-order ratio of hexanoyl sphingomyelin activation according to linear regression fitting was as follows: $y = 7.1494x - 1.5398$, where y is the activation ratio and x is the sphingomyelin concentration ($r^2 = 0.9978$). RdRp activation had almost plateaued at 2 μM hexanoyl sphingomyelin. The activation kinetics of JFH1 (2a) and J6CF (2a) RdRps in egg yolk sphingomyelin were biphasic and plateaued at 0.01 mg/ml. Those of RMT (1a) and H77 (1a) RdRps in hexanoyl sphingomyelin were also biphasic and plateaued at 2 μM. The curve of the first order was fitted by linear regression. The molar ratio of RdRp to hexanoyl sphingomyelin at its plateau was calculated as 1:20.

Because RdRp activation had almost plateaued at 2 μM hexanoyl sphingomyelin, we compared the effect of sphingomyelin on 100 M concentrations of RNA polymerases of the HCV 1a, 1b, and 2a genotypes using 2 μM hexanoyl sphingomyelin (Fig. 1E and Table 1).

Helix-turn-helix structure for sphingomyelin binding and activation. Sphingomyelin binds to the SBD peptide (see HCV SBD in Fig. 7) (29). Initially, we tested whether SBD was the sphingomyelin binding site in HCV RdRp by ELISA (Fig. 2A and Table 1). When the L245 and I253 residues of the SBD peptide were mutated to A, sphingomyelin binding activity was lost (29). We introduced the same mutations in HCV HCR6 (1b) RdRp and purified HCR6 (1b) RdRp with mutations L245A, I253A, and L245A/I253A. Because the C-terminal His-tagged HCR6 RdRp(L245A/I253A) was not soluble, it was solubilized by tagging of glutathione *S*-transferase (GST) sequence at the N terminus but lost polymerase activity. As the L245A/I253A mutant had lost its polymerase activity, polymerase activation was tested only for L245A and I253A (Fig. 2B and Table 1). These results confirmed that SBD located in the finger domain (residues 230E to 263G) successfully achieved sphingomyelin binding in HCV RdRp and that sphingomyelin did not bind to the SBD when the helix-turn-helix structure had been destroyed by the L245A or I253A mutation (29).

The sphingomyelin binding activities of genotype 1a and 2a RdRps were also tested (Fig. 2 and Table 1). Both JFH1 and J6CF were tested for genotype 2a because J6CF (2a) RdRp had an additional amino acid difference at position 241 in the SBD, and its sphingomyelin binding activity was very low (Fig. 2A and 7A; Table 1). J6CF (2a) RdRp(R241Q) showed the same sphingomyelin binding activity as HCR6 (1b) RdRp wt, indicating that 241Q was the critical amino acid for sphingomyelin binding. J6CF (2a) RdRp(S244D) and RdRp(R241Q/S244D) also showed higher sphingomyelin binding activity

TABLE 1. Summary of sphingomyelin activation of HCV RNA polymerase activities

Parameter	Value for the parameter by RdRp genotype, strain, and variant[a]																				
	1b							1a						2a							
	HCR6									H77		J6CF				JFH1					
	wt	L245A	I253A	L245A/I253A	D244S	NN	Con1	RMT	wt	A238S/Q248E	wt	R241Q	S244D	R241Q/S244D	wt	A242C	S244D	A242C/S244D	T251Q
SM binding (%)[b]	100	24.3	30.8	15.5	78.7	93.4	117	144	86.7	82.5	19.3	118	53.1	80.2	70.4	75.5	93.1	92.4	80.7
Activation of polymerase (*n*-fold)[c]	13.0 (11.2)[d]	(2.8)[d]	(2.5)[d]	ND	3.6	7.9	7.9	3.0	2.0	8.1	2.3	4.3	5.6	3.4	1.6	1.0	3.1	4.4	1.8
Activation of RNA binding (*n*-fold)[c]	4.5	2.6	1.7	ND	1.9	ND	ND	ND	1.4	3.3	1.5	3.6	3.2	1.7	1.3	ND	ND	1.4	ND

[a] Numbers were averaged from three independent experiments. ND, not done.
[b] Egg yolk sphingomyelin (SM; 250 ng) was used.
[c] Hexanoyl sphingomyelin (2 μM) was used.
[d] Egg yolk sphingomyelin (0.01 mg/ml) was used.

than the wt ($P < 0.001$) but lower binding than the R241Q mutant. However, S244D showed higher RdRp activation than R241Q ($P < 0.005$), while the RdRp activation ratio of the double mutant (R241Q/S244D) was lower than that of S244D or R241Q, although all of them activated RdRp with sphingomyelin ($P < 0.005$) (Fig. 2A and C and Table 1). For JFH1, when the JFH1 RdRp SBD was modified (A242C/S244D) to allow it to bind with more sphingomyelin than the wt ($P < 0.005$), the mutant JFH1 RdRp(A242C/S244D) was activated more than the wt by sphingomyelin ($P < 0.005$) (Fig. 2A and C; Table 1). The sphingomyelin binding activity of JFH1 RdRp(T251Q) was 80.7% of that of HCR6 (1b), and its activation ratio was 1.8-fold. These results agree that SBD is both the sphingomyelin activation and binding domain and that the domains for these two activities are somehow different.

We determined which amino acid, 242C or 244D, enhanced sphingomyelin binding by comparing HCR6 (1b) and JFH1 (2a) RdRps. Sphingomyelin binding of HCR6 (1b) RdRp(D244S) was 79% of that of the wt ($P < 0.005$) (Fig. 2A and Table 1), and its activation by sphingomyelin was only 3.6-fold (Fig. 2C and Table 1). The sphingomyelin binding of JFH1 (2a) RdRp(A242C) and RdRp(S244D) increased to 75.5% and 93.1%, respectively, of HCR6 (1b) RdRp wt (Fig. 2A and Table 1). This was significantly higher than that of JFH1 (2a) RdRp wt ($P < 0.005$), and the sphingomyelin activation of JFH1 (2a) RdRp(A242C) and RdRp(S244D) was increased 1.0-fold and 3.1-fold, respectively ($P < 0.005$) (Fig. 2C and Table 1). From these mutation analyses of the J6CF and JFH1 RdRps, we concluded that 244D enhanced sphingomyelin binding and RdRp activation.

HCV 1a RdRps were not activated even though sphingomyelin bound to them (Fig. 1E and 2A and Table 1). We then tried to elucidate the domains responsible for sphingomyelin activation. There are 14 amino acids (residues 19, 25, 81, 111, 120, 131, 184, 270, 272, 329, 436, 464, 487, and 540) unique to genotype 1a RdRp in the region of residues 1 to 570 and two amino acid differences unique to 1a RdRp in SBD, i.e., 238A and 248Q (see Fig. 6A). Initially, we focused on the SBD and introduced the A238S and Q248E mutations into the H77 (2a) RdRp SBD (Fig. 2A and D and Table 1). The sphingomyelin binding activity of H77 (2a) RdRp(A238S/Q248E) was similar to that of H77 (2a) RdRp wt. The sphingomyelin activation ratio of H77 (2a) RdRp(A238S/Q248E) was increased 8.1-fold, leading us to conclude that these mutations are essential to sphingomyelin activation.

Effect of lipids on HCV RNA polymerase activity. In order to elucidate the structure of the lipids involved in activation of HCV RdRp, D-lactosyl-β-1,1′-*N*-octanoyl-D-*erythro*-sphingosine [C_8-lactosyl(β) ceramide], D-glucosyl-β1-17-N-octanoyl-D-*erythro*-sphingosine (C_8-β-D-glucosyl ceramide), *N*-hexanol-D-*erythro*-sphingosine (C_6-ceramide), and cholesterol were tested for their abilities to activate RdRp. The relative polymerase activities of 100 nM HCV HCR6 (1b) RdRp activated with 0.01 mg/ml egg yolk sphingomyelin, 2 μM hexanoyl sphingomyelin, 8 μM C_8-lactosyl(β) ceramide, 12 μM C_8-β-D-glucosyl ceramide, 12 μM C_6-ceramide, and 0.02 mg/ml cholesterol were 11.2, 13.0, 5.66, 4.19, 1.12, and 2.25 of that without lipids, respectively (Fig. 3A). The amount of lipids that gave the maximum activation was calculated from the kinetics of the lipids bound to HCR6 (1b) and JFH1 (2a) RdRps (Fig. 3B and

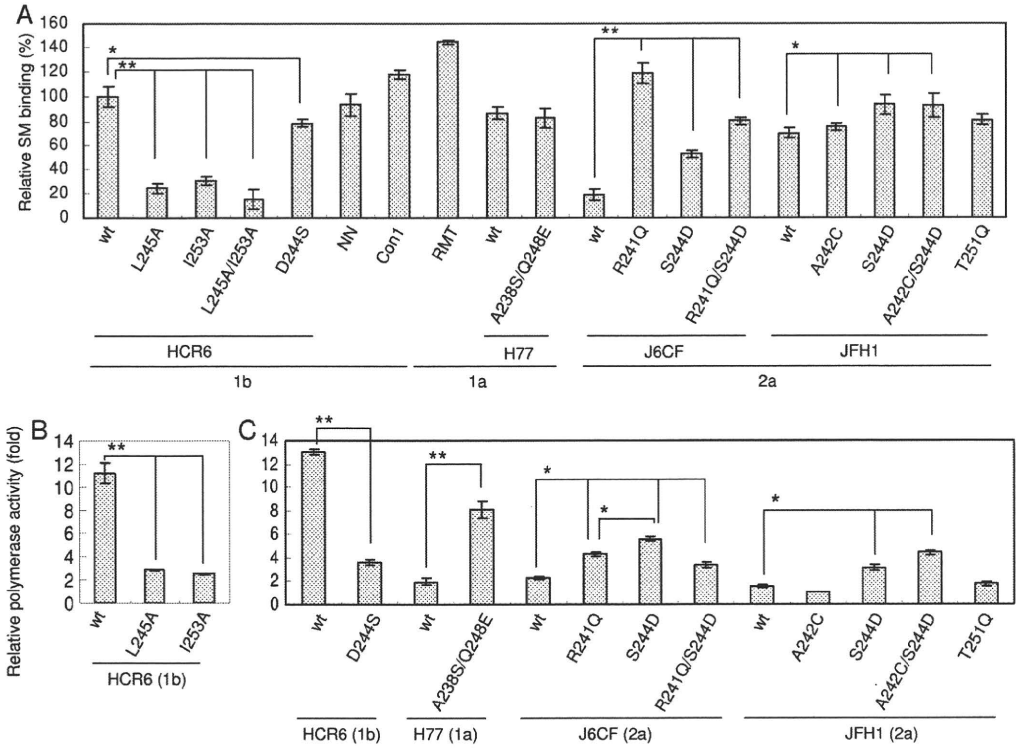

FIG. 2. Sphingomyelin binding and activation of HCV RNA polymerase sphingomyelin binding domain mutants. Names of RdRps are indicated below the graphs. (A) Egg yolk sphingomyelin (SM) binding activity relative to that of HCR6 (1b) RdRp wt. Mean ± standard deviation of the binding was calculated from three independent experiments. (B) Egg yolk sphingomyelin activation of HCR6 (1b) RdRps. RdRps (100 nM) were incubated with or without 0.01 mg/ml egg yolk sphingomyelin. (C) Hexanoyl sphingomyelin activation of the RdRps (RdRp names are indicated below the graphs). HCV RdRps (100 nM) were incubated with or without 2 μM hexanoyl sphingomyelin. The mean ± standard deviation of the activation ratio was calculated from three independent experiments. *, $P < 0.005$; ** $P < 0.001$.

C). C_8-lactosyl(β) ceramide and C_8-β-D-glucosyl ceramide activated HCR6 (1b) RdRp compared with the linear regression kinetics of the reaction with hexanoyl sphingomyelin as it plateaued (Fig. 1C and 3B). Cholesterol activated HCR6 (1b) RdRp slightly but did not activate JFH1 (2a) RdRp (Fig. 3C). We therefore concluded that the phosphocholine of sphingomyelin bound to the SBD of HCV RdRp because the order of HCV RdRp activation was hexanoyl sphingomyelin > C_8-lactosyl(β) ceramide > C_8-β-D-glucosyl ceramide, and C_6-ceramide did not activate HCV HCR6 (1b) RdRp. The polarity of the phosphocholine of sphingomyelin is important for HCV RdRp activation (see Fig. S5 in the supplemental material).

In order to test whether phosphocholine activated HCV RdRp (Fig. 3D), HCR6 (1b) RdRp was incubated with 0.4, 2, 20, 100, and 400 μg and 2, 4, 11, 54, and 100 mg of phosphocholine. Up to 400 μg of phosphocholine did not affect RdRp activity, but more than 2 mg of phosphocholine inhibited RdRp activity.

Effect of sphingomyelin on the template RNA binding of HCV RNA polymerase. The mechanism of HCV RdRp activation was analyzed. RNA polymerase changes its conformation throughout the different transcription steps, and template binding is the first step of transcription (9). Therefore, the effect of sphingomyelin on template RNA binding activity was tested (Fig. 4A and Table 1). Sphingomyelin enhanced the template RNA binding of HCR6 (1b) RdRp wt but not that of JFH1 (2a), H6CF (2a), or H77 (1a) wt RdRp. When the A238S/Q248E mutation was introduced into H77 (1a) RdRp, the RNA binding was enhanced. J6CF (2a) RdRp R241Q and S244D mutants showed similar enhancement of RNA binding, but the R241Q/S244D double mutant did not. The activation effect of RNA binding of HCR6 (1b) RdRp mutants L245A, I253A, and D244S was lower than that of RdRp wt. JFH1 (2a) RdRp wt and RdRp(A242C/S244D) showed similar RNA binding activation levels. Based on a comparison of the sphingomyelin activation of HCR6 (1b) RdRp wt and its mutants which lost sphingomyelin binding with J6CF (2a) RdRp wt and the R241Q and S244D mutants and H77 (1a) RdRp wt and the A238S/Q248E mutant, we concluded that polymerase activation by sphingomyelin was induced mainly via activation of the template RNA binding of RdRp. RNA binding activity of JFH1 (2a) RdRp wt and RdRp(A242C/S244D) was almost saturated because RNA binding of these RdRps was not activated by sphingomyelin (see Fig. S4 in the supplemental material).

HCV RdRp has to be bound with sphingomyelin before or at the same time as it binds to template RNA. After RdRp had bound to the template RNA, sphingomyelin did not enhance template RNA binding strongly (Fig. 4B).

Effect of the sphingomyelin binding domain mutations for HCV replicon activity with myriocin. In order to confirm sphingomyelin activation of HCV polymerase activity in a viral replication system, HCV replicon activity of the loss-of-function mutant HCV NN (1b) NS5B(D244S) and the gain-of-

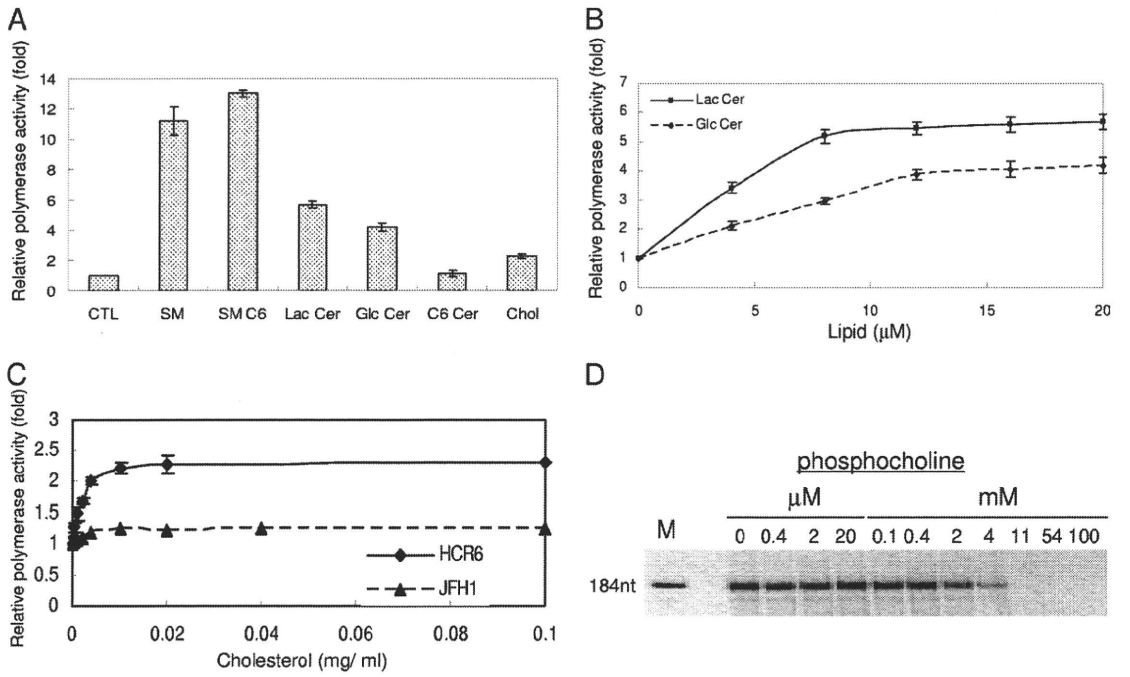

FIG. 3. HCV RNA polymerase activation effect of lipids. (A) Lipid activation of HCR6 (1b) RdRp wt. HCV HCR6 (1b) RdRp wt (100 nM) was incubated with or without (control [CTL]) 0.01 mg/ml egg yolk sphingomyelin (SM), 2 μM hexanoyl sphingomyelin (SM C6), 8 μM C_8-lactosyl(β) ceramide (Lac Cer), 12 μM C_8-β-D-glucosyl ceramide (Glc Cer), 12 μM C_6-ceramide (C6 Cer), or 0.02 mg/ml cholesterol (chol). (B) Activation kinetics of C_8-lactosyl(β) ceramide (Lac Cer) and C_8-β-D-glucosyl ceramide (Glc Cer) on HCR6 (1) RdRp. (C) Activation kinetics of cholesterol on HCR6 (1b) and JFH1 (12a) RdRps. (D) The effect of phosphocholine on HCR6 (1b) RdRp. The mean ± standard deviation of the activation ratio was calculated from three independent experiments.

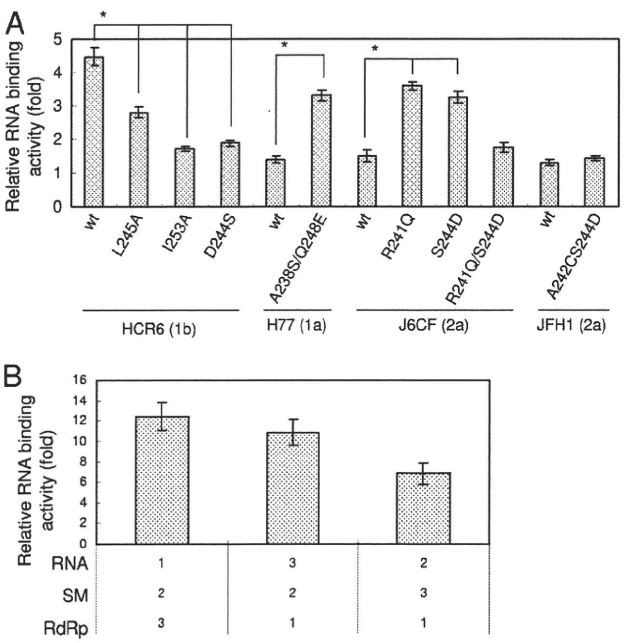

FIG. 4. Sphingomyelin activation of the RNA binding activity of HCV RNA polymerase. (A) Sphingomyelin activation of RNA filter binding of HCV RdRps (RdRp names are indicated below the graph). RdRps and ^{32}P-labeled RNA template (SL12-1S) were incubated with or without egg yolk sphingomyelin (SM), before filtration. (B) Effect of the order of sphingomyelin treatment. Numbers below the graph indicate the order in which the reagents were added. The graph represents the ratio to RNA binding without sphingomyelin. The mean ± standard deviation of the activation ratio was calculated from three independent experiments. *, $P < 0.01$.

function mutants H77 (1a) NS5B(A238S/Q248E) and JFH1 (2a) NS5B(A242C/S244D) were compared with 5 and 50 nM myriocin treatment for 72 h (Fig. 5).

First, HCV replicon activity was compared as the relative luciferase activity (Fig. 5A). Both JFH1 (2a) wt and NS5B(A242C/S244D) replicons showed similar and strong replicon activity ($133 \times 10^3 \pm 12 \times 10^3$ and $138 \times 10^3 \pm 8.5 \times 10^3$, respectively). JFH1 (2a) wt replicon was resistant to myriocin treatment, as reported by Aizaki et al. using other SPT inhibitors (3). The JFH1 (2a) NS5B(A242C/S244D) replicon became sensitive to myriocin but still showed higher replicon activity than NN (1b) or H77 (1a) replicons even at 50 nM myriocin.

To analyze the effect of mutations precisely, the replicon activity relative to each wt strain was compared (Fig. 5B). The JFH1 (2a) wt replicon with 50 nM myriocin showed the same luciferase activity as the wt without myriocin (102% ± 9.6%). JFH1 (2a) NS5B(A242C/S244D) replicon activity was the same as that of the wt without myriocin (103% ± 12%); with 5 nM myriocin it was 84.1% ± 6.6% of the wt level, but with 50 nM myriocin it was 70.3% ± 5.3% of the wt level, which was significantly lower ($P < 0.01$). NN (1b) wt replicon activity was 45.3% ± 6.6% with 5 nM myriocin and 21.7% ± 2.9% with 50 nM myriocin relative to the wt level without myriocin. NN (1b) NS5B(D244S) replicon activity was 72.2% ± 12% without myriocin ($P < 0.05$), 44.0% ± 7.4% with 5 nM myriocin, and 38.1% ± 4.2% with 50 nM myriocin relative to wt level without myriocin, which was significantly higher ($P < 0.01$). Thus, NN (1b) NS5B(D244S) showed lower replicon activity than the wt

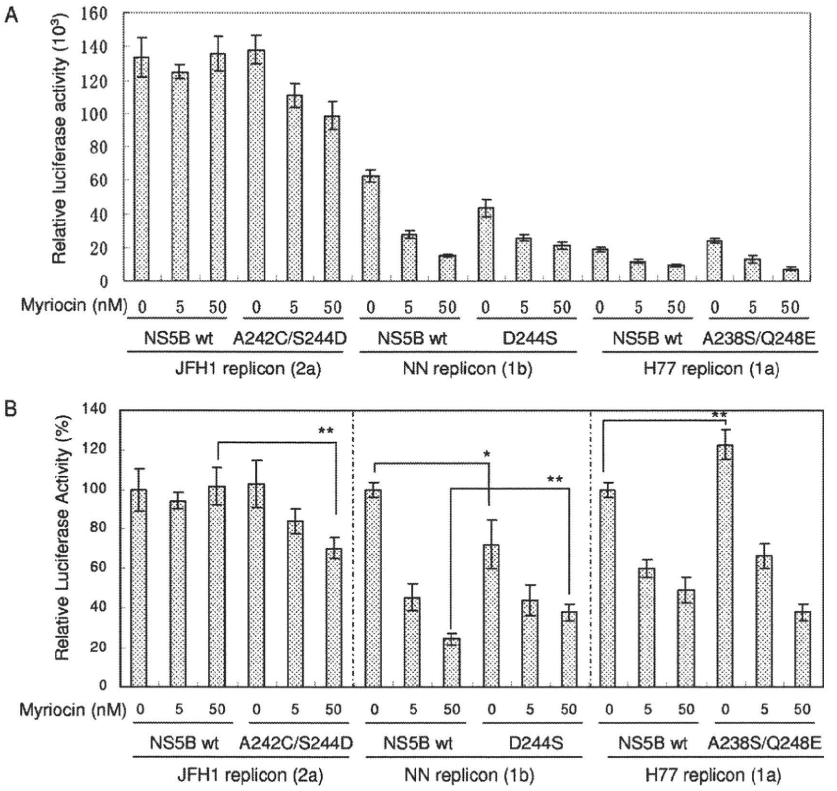

FIG. 5. Myriocin inhibition of HCV replicon activity. Huh7.5.1 cells were incubated with myriocin after transfection with the HCV replicons indicated below the graphs. Means ± standard deviations of the relative luciferase activity at 72 h after myriocin treatment compared to activity at 4 h after transfection (A) and to that of each wt without myriocin (B) were calculated from three independent measurements. *, $P < 0.05$; ** $P < 0.01$.

and was less sensitive to myriocin than the wt. H77 (1a) wt replicon activity was 59.9% ± 4.2% with 5 nM myriocin and 49.2% ± 6.4% with 50 nM myriocin relative to the wt level without myriocin. H77 (1a) NS5B(A238S/Q248E) replicon activity was 123% ± 7.1% without myriocin ($P < 0.01$), 66.1% ± 6.3% with 5 nM myriocin, and 38.0% ± 4.1% with 50 nM myriocin relative to wt level without myriocin. Both H77 (1a) wt and NS5B(A238S/Q248E) replicons were sensitive to myriocin, and the replicon activity of NS5B(A238S/Q248E) was higher than that of the wt.

JFH1 (2a) RdRp(A242C/S244D) localized in the DRM fractions. Myriocin sensitivity of JFH1 (2a) NS5B(A242C/S244D) replicon indicates the importance of 244D in JFH1 NS5B for sphingomyelin binding. To further confirm the role of 244D for recruitment of HCV RdRp to the detergent-resistant membrane (DRM), where the HCV replication complex exists, we compared the distribution of NS5A and NS5B of JFH1 (2a) wt and NS5B(A242C/S244D) in their replicon cells by sucrose density gradient centrifugation of the DRM (Fig. 6). NS5A proteins of both JFH1 (2a) wt and NS5B(A242C/S244D) replicons localized in the DRM fraction where caveolin-2 was present (11, 27), but most of NS5B wt localized in the Triton-soluble fractions. NS5B of JFH1 (2a) NS5B(A242C/S244D) replicon was shifted to the DRM fraction from the soluble fraction. The shift of NS5B(A242C/S244D) localization into the DRM demonstrated that SBD was the DRM localization domain of NS5B and that residue 244D was important for this localization.

DISCUSSION

Hepatitis C virus is an envelope virus, and the lipid components of the virion play important roles in HCV infectivity and virion assembly (3, 15, 20, 24). HCV replication complexes localize in lipid raft structures/DRMs in the membrane frac-

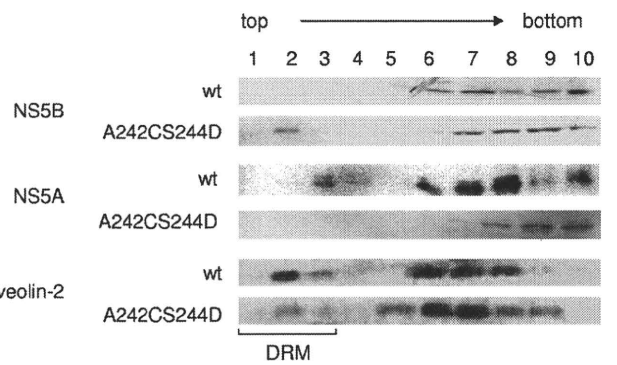

FIG. 6. Membrane floating assay of JFH1 wt and NS5B(A242C/S244D) replicon cells. The PNS fractions of HCV JFH1 (2a) wt and NS5B(A242C/S244D) replicon cells were treated with 1% Triton X-100 in TNE buffer for 30 min at 4°C and subjected to 10 to 40% sucrose gradient centrifugation in TNE buffer. Each fraction was subjected to 10% SDS-PAGE, followed by Western blotting with anti-NS5A, -NS5B, and -caveolin-2 antibodies. Fractions are numbered as indicated at the top of the panel. The DRM fractions (fractions 1 to 3) are indicated.

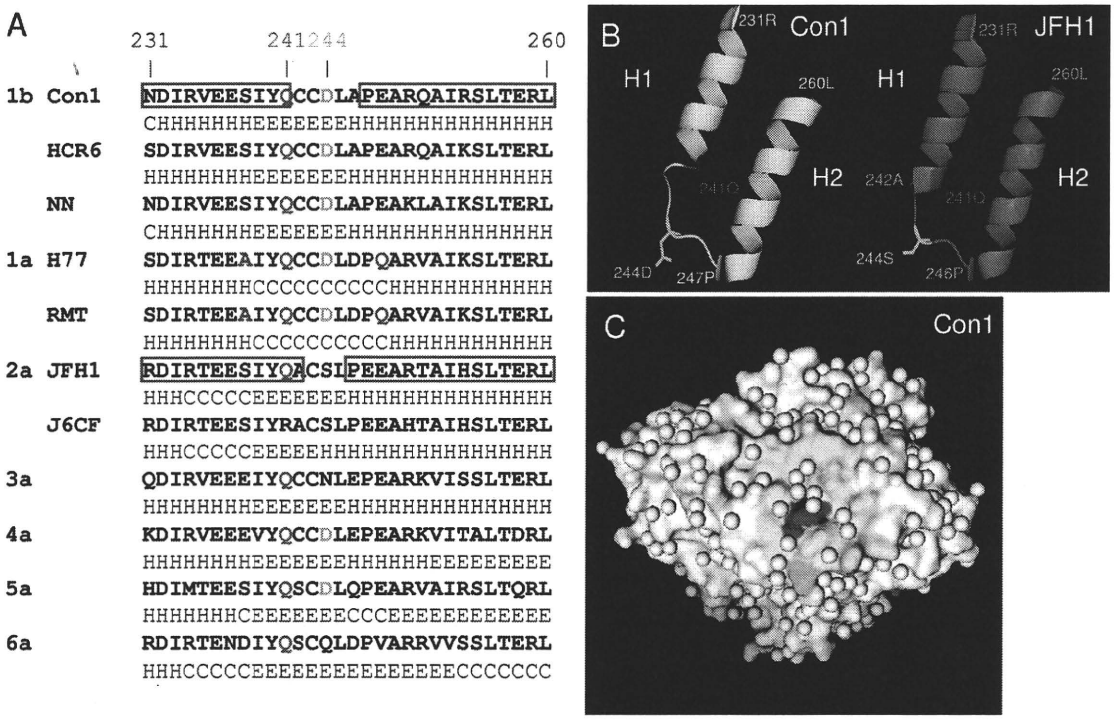

FIG. 7. Sphingomyelin binding domain (SBD) of HCV RNA polymerase. (A) The SBDs (231N to 260L) of HCV RdRps are aligned together with their secondary structure predicted by the Chou-Fasman program (10). The predicted secondary structure is indicated below the sequence as follows: H, α-helix; E, β-sheet; and C, coil. The α-helix structures of HCV Con1 (1b) RdRp and JFH1 (2a) RdRp are boxed in red. Residues 241Q and 244D are indicated in red and green, respectively. The 238A and 248E of the H77 and RMT (1a) RdRps are indicated in purple. GenBank accession numbers of HCV genotypes 3a, 4a, 5a, and 6a are GU814263 (12), GU814265 (12), Y13184 (8), and Y12083 (1), respectively. (B) Comparison of the SBDs of HCV Con1 (1b) (yellow) and JFH1 (2a) RdRps (magenta). The starting and ending amino acids of H1 and H2 are indicated. The sphingomyelin binding site, 241Q, is indicated in red, and 244D of Con1 (1b) and 244S of JFH1 (2a) RdRp are indicated in green. (C) Surface model of HCV Con1 (1b) RdRp. SBD is indicated in yellow, and 241Q and 244D are indicated in red and green, respectively. The structures of the Con1 and JFH1 RdRps were constructed by PyMOL, version 1.1.1 (http://www.pymol.org/). PDB numbers of Con1 (1b) RdRp and JFH1 (2a) RdRp are 3FQL (14) and 3I5K (31), respectively.

tions of subgenomic replicon cells (30). Lipid rafts are composed mainly of sphingomyelin, cholesterol, and glycosphingolipids. Most reports regarding the relationship between lipids and HCV have examined virion assembly, infectivity, and the localization of HCV, but their biochemical interactions have not been reported. Our findings clearly demonstrate that sphingomyelin plays an important role not only in HCV replication complex formation and its localization but also in HCV RdRp activity.

The helix-turn-helix structure of the SBD (residues 230 to 263), which is located between RNA polymerase motifs A and B, has been proposed as the sphingomyelin binding domain of HCV RdRp (29). We compared the SBD of Con1 (1b) (Protein Data Bank [PDB] 3FQL) (14) and JFH1 (2a) (PDB 3I5K) (31) and the secondary structure of the amino acids (201 to 290) in the SBD predicted by the Chou-Fasman program (10) (Fig. 7; see also Fig. S5 in the supplemental material) because the helix structures of the SBD of Con1 (helix 1 [H1], 231N to 241Q; helix 2 [H2], 247A to 260L) and JFH1 (H1, 231R to 242A; H2, 246P to 260L) RdRp fit with those predicted by the Chou-Fasman program. The structures contributing to sphingomyelin binding and activation are H1 and H2 and the junction (turn) between the two helix structures that are similar to the human immunodeficiency virus (HIV) gp120 V3 domain, prion protein (PrP), and β-amyloid peptide (13, 22). Although Con1 (1b) RdRp has a shorter helix structure than JFH1 (2a) RdRp (Fig. 6B), the structures of their SBDs are very similar (Fig. 7; see also Fig. S5). When the helix-turn-helix structure of the SBD was destroyed (HCR6 genotype 1b RdRp mutants L245A and I253A), the RdRp lost sphingomyelin binding activity and lost its activation (Fig. 2).

In order to study the structure-function relationship of the SBD and sphingomyelin, we compared the SBD of genotype 1a, 1b and 2a RdRps and particularly focused on residue 244D in the turn and residues 241Q and 238S/248E in the helix domains. The polar amino acid 241Q and the negatively charged 244D of Con1 (1b) RdRp located on the surface of the RdRp molecule bind and interact with the positively charged choline residue of sphingomyelin (Fig. 7C; see also Fig. S5 in the supplemental material). The positively charged 241R repels the choline residue of sphingomyelin, and as a result, J6CF (a) RdRp wt did not bind to sphingomyelin. J6CF (2a) RdRp(R241Q) showed almost the same sphingomyelin binding activity as HCR6 (1b) RdRp wt. This ionic interaction between SBD and sphingomyelin agrees with the activation of lipids with different sphingosine structures and fatty acid chains (Fig. 3A). JFH1 (2a) RdRp does not interact well with sphingomyelin because it does not have the negatively charged

amino acids at the tip of its turn structure. Once its 244S was changed to D, more sphingomyelin bound to JFH1 (2a) RdRp and activated the RdRp (Fig. 2A and C). The reason for the low activation of J6CF (2a) RdRp(R241Q/S244D) is not clear. Sometimes mutations affect the entire conformation of the molecule. In conclusion, from the comparison of sphingomyelin binding and activation of HCR6 (1b), J6CF (2a), and JFH1 (2a) RdRp SBD mutants, 241Q is the essential amino acid for sphingomyelin binding in the SBD. Amino acid 244D enhanced both binding and RdRp activation.

The *in vitro* sphingomyelin binding and RdRp activation experiments indicate that sphingomyelin binding and its RdRp activation are different biochemical reactions because we found controversial activation rates for sphingomyelin binding and RdRp activation among J6CF (2a) RdRp mutants (Fig. 2). The relationship between sphingomyelin binding and the activation of polymerase activity was studied by comparing genotype 1b and 1a RdRps, both of which bind to sphingomyelin (Fig. 2). However, 1a RdRp is not activated by sphingomyelin because both of the helix structures of 1a RdRp are probably terminated at 238A and 248Q, making its helix structures shorter than those of 1b RdRp (Fig. 6A). The length of the helix structure may be essential for sphingomyelin activation because RdRp changes its structure to bind to template RNA when sphingomyelin binds to SBD (Fig. 4).

HCV RdRp changes its conformations at the early stages of transcription initiation, including the template RNA binding step (6, 9). Sphingomyelin binding is likely to change the conformation of 1b RdRp to recruit template RNA and initiate transcription efficiently. Comparison of the activation ratio of RNA binding and polymerase activity of 1b RdRp, J6CF (2a) RdRp wt and R241Q and S244D mutants, and JFH1 (2a) RdRp wt and mutant A242C/S244D suggests that steps other than RNA binding are also likely to be activated by sphingomyelin.

From a kinetic analysis of sphingomyelin activation (Fig. 1C and D), 20 sphingomyelin molecules are estimated to interact with the SBD of RdRp and activate it because sphingomyelin activation plateaued at 20 sphingomyelin molecules per HCV RdRp molecule. It is not clear whether 20 sphingomyelin molecules form a micelle or a layer structure. However, the structure of sphingomyelin is important for the activation of HCV RdRp because phosphocholine did not activate the RdRp (Fig. 3D).

To confirm these biochemical findings in HCV replication, we tested the effect of SBD mutations in HCV replicon systems with the SPT inhibitor myriocin (Fig. 5) (4, 33) because NA255 was not available. The loss-of-function mutant, HCV NN (1b) NS5B(D244S), showed lower replicon activity than NN (1b) wt and more resistance to 50 nM myriocin, which did not affect the viability of cells (4, 33), than the wt. The gain-of-function mutant, H77 (1a) NS5B(A238S/Q248E), showed higher replicon activity than H77 wt and retained myriocin sensitivity because it had the sphingomyelin binding sites 241Q and 244D. At 50 nM myriocin, another gain-of-function mutant, JFH1 (2a) NS5B(A242C/S244D), was inhibited although its activity was the same as that of JFH1 (2a) wt without myriocin because the JFH1 wt replicon had high replicon activity without myriocin (Fig. 5A). The JFH1 replicon activity may be maximal in the system; therefore, the JFH1 (2a) NS5B(A242C/S244D) replicon did not show higher activity than JFH1 (2a) wt without myriocin while H77 (1a) NS5B(A238S/Q248E) showed higher replicon activity than H77 wt.

The binding and RdRp activation activity of the amino acid 244 mutants by sphingomyelin did not differ greatly from the wt *in vitro*. However, the myriocin sensitivity of JFH1 (2a) NS5B(S244D) was demonstrated clearly. That of H77 (1a) NS5B(A238S/Q248E) indicated that sphingomyelin binding was the target of myriocin inhibition, not the sphingomyelin activation of RdRp. These data confirm the importance of 241Q, 244D, and the helix structure in SBD for HCV replication in the cells.

Sphingomyelin is the major component of the lipid raft structure/DRM where the HCV genome replicates. To confirm that the SBD is the membrane binding site of HCV RdRp, we analyzed the localization of NS5B of JFH1 (2a) wt and NS5B(A242C/S244D) replicons by membrane floating assay (Fig. 6). JFH1 (2a) NS5B wt did not localize in the DRM. However, the localization of NS5B of the JFH1 (2a) NS5B(A242C/S244D) replicon shifted to the DRM from the soluble fractions. Previously, HCV NS5B was believed to localize in the DRM by its C-terminal hydrophobic sequences (21). However, our data demonstrate that the SBD is the membrane localization domain of HCV NS5B, which agrees with the myriocin sensitivity of JFH1 (2a) NS5B(A242C/S244D) replicons (Fig. 5) and the release of HCV 1b NS5B from the DRM by another SPT inhibitor, NA255 (29).

This is the first report of RNA polymerase activation by lipids. Twenty sphingomyelin molecules interact with SBD, particularly with residues 241Q and 244D of HCV (1b) RdRp, and change the conformation of the RdRp in order to recruit RNA templates. At the same time, HCV RdRp molecules may be aligned on the sphingomyelin layer formed via interactions between the hydrocarbon chains of sphingosine and fatty acids via placement of their SBD into the layer (Fig. 7C). Consistent with previous research (3, 23, 37), our findings explain why the inhibitors of the sphingolipid biosynthetic pathway influence subgenomic replicons derived from HCV genotypes 1a and 1b but not those derived from JFH1 (2a) (Fig. 5). Most HCV isolates have 241Q in NS5B, and some of them also have 244D (Fig. 7A). These sphingomyelin interactions are new targets for the treatment of HCV.

ACKNOWLEDGMENTS

We thank C. Rice and R. Bartenshlager for the HCV H77 and Con1 plasmids, respectively. We also thank F. Chisari for Huh7.5.1 and Huh7/src cells.

This work was supported by a grant-in-aid from the Chinese Academy of Sciences (O514P51131 and KSCX1-YW-10), the Chinese 973 project (2009CB522504), and the Chinese National Science and Technology Major Project (2008ZX10002-014).

REFERENCES

1. **Adams, N. J., R. W. Chamberlain, L. A. Taylor, F. Davidson, C. K. Lin, R. M. Elliott, and P. Simmonds.** 1997. Complete coding sequence of hepatitis C virus genotype 6a. Biochem. Biophys. Res. Commun. **234**:393–396.
2. **Aizaki, H., K. J. Lee, V. M. Sung, H. Ishiko, and M. M. Lai.** 2004. Characterization of the hepatitis C virus RNA replication complex associated with lipid rafts. Virology **324**:450–461.
3. **Aizaki, H., K. Morikawa, M. Fukasawa, H. Hara, Y. Inoue, H. Tani, K. Saito, M. Nishijima, K. Hanada, Y. Matsuura, M. M. Lai, T. Miyamura, T. Wakita, and T. Suzuki.** 2008. Critical role of virion-associated cholesterol and sphingolipid in hepatitis C virus infection. J. Virol. **82**:5715–5724.
4. **Amemiya, F., S. Maekawa, Y. Itakura, A. Kanayama, A. Matsui, S. Takano, T. Yamaguchi, J. Itakura, T. Kitamura, T. Inoue, M. Sakamoto, K. Yamau-**

chi, S. Okada, A. Yamashita, N. Sakamoto, M. Itoh, and N. Enomoto. 2008. Targeting lipid metabolism in the treatment of hepatitis C virus infection. J. Infect. Dis. **197:**361–370.

5. **Binder, M., D. Quinkert, O. Bochkarova, R. Klein, N. Kezmic, R. Bartenschlager, and V. Lohmann.** 2007. Identification of determinants involved in initiation of hepatitis C virus RNA synthesis by using intergenotypic replicase chimeras. J. Virol. **81:**5270–5283.
6. **Biswal, B. K., M. M. Cherney, M. Wang, L. Chan, C. G. Yannopoulos, D. Bilimoria, O. Nicolas, J. Bedard, and M. N. James.** 2005. Crystal structures of the RNA-dependent RNA polymerase genotype 2a of hepatitis C virus reveal two conformations and suggest mechanisms of inhibition by non-nucleoside inhibitors. J. Biol. Chem. **280:**18202–18210.
7. **Blight, K. J., J. A. McKeating, J. Marcotrigiano, and C. M. Rice.** 2003. Efficient replication of hepatitis C virus genotype 1a RNAs in cell culture. J. Virol. **77:**3181–3190.
8. **Chamberlain, R. W., N. J. Adams, L. A. Taylor, P. Simmonds, and R. M. Elliott.** 1997. The complete coding sequence of hepatitis C virus genotype 5a, the predominant genotype in South Africa. Biochem. Biophys. Res. Commun. **236:**44–49.
9. **Chinnaswamy, S., I. Yarbrough, S. Palaninathan, C. T. Kumar, V. Vijayaraghavan, B. Demeler, S. M. Lemon, J. C. Sacchettini, and C. C. Kao.** 2008. A locking mechanism regulates RNA synthesis and host protein interaction by the hepatitis C virus polymerase. J. Biol. Chem. **283:**20535–20546.
10. **Chou, P. Y., and G. D. Fasman.** 1974. Prediction of protein conformation. Biochemistry **13:**222–245.
11. **Fujimoto, T., H. Kogo, K. Ishiguro, K. Tauchi, and R. Nomura.** 2001. Caveolin-2 is targeted to lipid droplets, a new "membrane domain" in the cell. J. Cell Biol. **152:**1079–1085.
12. **Gottwein, J. M., T. K. Scheel, B. Callendret, Y. P. Li, H. B. Eccleston, R. E. Engle, S. Govindarajan, W. Satterfield, R. H. Purcell, C. M. Walker, and J. Bukh.** Novel infectious cDNA clones of hepatitis C virus genotype 3a (strain S52) and 4a (strain ED43): genetic analyses and *in vivo* pathogenesis studies. J. Virol. **84:**5277–5293.
13. **Hammache, D., G. Pieroni, N. Yahi, O. Delezay, N. Koch, H. Lafont, C. Tamalet, and J. Fantini.** 1998. Specific interaction of HIV-1 and HIV-2 surface envelope glycoproteins with monolayers of galactosylceramide and ganglioside GM3. J. Biol. Chem. **273:**7967–7971.
14. **Hang, J. Q., Y. Yang, S. F. Harris, V. Leveque, H. J. Whittington, S. Rajyaguru, G. Ao-Ieong, M. F. McCown, A. Wong, A. M. Giannetti, S. Le Pogam, F. Talamas, N. Cammack, I. Najera, and K. Klumpp.** 2009. Slow binding inhibition and mechanism of resistance of non-nucleoside polymerase inhibitors of hepatitis C virus. J. Biol. Chem. **284:**15517–15529.
15. **Huang, H., F. Sun, D. M. Owen, W. Li, Y. Chen, M. Gale, Jr., and J. Ye.** 2007. Hepatitis C virus production by human hepatocytes dependent on assembly and secretion of very low-density lipoproteins. Proc. Natl. Acad. Sci. U. S. A. **104:**5848–5853.
16. **Ishii, N., K. Watashi, T. Hishiki, K. Goto, D. Inoue, M. Hijikata, T. Wakita, N. Kato, and K. Shimotohno.** 2006. Diverse effects of cyclosporine on hepatitis C virus strain replication. J. Virol. **80:**4510–4520.
17. **Kashiwagi, T., K. Hara, M. Kohara, K. Kohara, J. Iwahashi, N. Hamada, H. Yoshino, and T. Toyoda.** 2002. Kinetic analysis of C-terminally truncated RNA-dependent RNA polymerase of hepatitis C virus. Biochem. Biophys. Res. Commun. **290:**1188–1194.
18. **Kato, T., T. Date, M. Miyamoto, A. Furusaka, K. Tokushige, M. Mizokami, and T. Wakita.** 2003. Efficient replication of the genotype 2a hepatitis C virus subgenomic replicon. Gastroenterology **125:**1808–1817.
19. **Kiyosawa, K., T. Sodeyama, E. Tanaka, Y. Gibo, K. Yoshizawa, Y. Nakano, S. Furuta, Y. Akahane, K. Nishioka, R. H. Purcell, et al.** 1990. Interrelationship of blood transfusion, non-A, non-B hepatitis and hepatocellular carcinoma: analysis by detection of antibody to hepatitis C virus. Hepatology **12:**671–675.
20. **Lambot, M., S. Fretier, A. Op De Beeck, B. Quatannens, S. Lestavel, V. Clavey, and J. Dubuisson.** 2002. Reconstitution of hepatitis C virus envelope glycoproteins into liposomes as a surrogate model to study virus attachment. J. Biol. Chem. **277:**20625–20630.
21. **Lemon, S., C. Walker, M. Alter, and M. Yi.** 2007. Hepatitis C virus, p. 1253–1304. *In* D. M. Knipe, P. M. Howley, D. E. Griffin, R. A. Lamb, M. A. Martin, B. Roizman, and S. E. Straus (ed.), Fields virology, 5th ed. Lippincott Williams & Wilkins, Philadelphia, PA.
22. **Mahfoud, R., N. Garmy, M. Maresca, N. Yahi, A. Puigserver, and J. Fantini.** 2002. Identification of a common sphingolipid-binding domain in Alzheimer, prion, and HIV-1 proteins. J. Biol. Chem. **277:**11292–11296.
23. **Miyake, Y., Y. Kozutsumi, S. Nakamura, T. Fujita, and T. Kawasaki.** 1995. Serine palmitoyltransferase is the primary target of a sphingosine-like immunosuppressant, ISP-1/myriocin. Biochem. Biophys. Res. Commun. **211:**396–403.
24. **Miyanari, Y., K. Atsuzawa, N. Usuda, K. Watashi, T. Hishiki, M. Zayas, R. Bartenschlager, T. Wakita, M. Hijikata, and K. Shimotohno.** 2007. The lipid droplet is an important organelle for hepatitis C virus production. Nat. Cell Biol. **9:**1089–1097.
25. **Murayama, A., T. Date, K. Morikawa, D. Akazawa, M. Miyamoto, M. Kaga, K. Ishii, T. Suzuki, T. Kato, M. Mizokami, and T. Wakita.** 2007. The NS3 helicase and NS5B-to-3′X regions are important for efficient hepatitis C virus strain JFH-1 replication in Huh7 cells. J. Virol. **81:**8030–8040.
26. **Murayama, A., L. Weng, T. Date, D. Akazawa, X. Tian, T. Suzuki, T. Kato, Y. Tanaka, M. Mizokami, T. Wakita, and T. Toyoda.** 2010. RNA polymerase activity and specific RNA structure are required for efficient HCV replication in cultured cells. PLoS Pathog. **6:**e1000885.
27. **Ostermeyer, A. G., J. M. Paci, Y. Zeng, D. M. Lublin, S. Munro, and D. A. Brown.** 2001. Accumulation of caveolin in the endoplasmic reticulum redirects the protein to lipid storage droplets. J. Cell Biol. **152:**1071–1078.
28. **Saito, I., T. Miyamura, A. Ohbayashi, H. Harada, T. Katayama, S. Kikuchi, Y. Watanabe, S. Koi, M. Onji, Y. Ohta, et al.** 1990. Hepatitis C virus infection is associated with the development of hepatocellular carcinoma. Proc. Natl. Acad. Sci. U. S. A. **87:**6547–6549.
29. **Sakamoto, H., K. Okamoto, M. Aoki, H. Kato, A. Katsume, A. Ohta, T. Tsukuda, N. Shimma, Y. Aoki, M. Arisawa, M. Kohara, and M. Sudoh.** 2005. Host sphingolipid biosynthesis as a target for hepatitis C virus therapy. Nat. Chem. Biol. **1:**333–337.
30. **Shi, S. T., K. J. Lee, H. Aizaki, S. B. Hwang, and M. M. Lai.** 2003. Hepatitis C virus RNA replication occurs on a detergent-resistant membrane that cofractionates with caveolin-2. J. Virol. **77:**4160–4168.
31. **Simister, P., M. Schmitt, M. Geitmann, O. Wicht, U. H. Danielson, R. Klein, S. Bressanelli, and V. Lohmann.** 2009. Structural and functional analysis of hepatitis C virus strain JFH1 polymerase. J. Virol. **83:**11926–11939.
32. **Tsukiyama-Kohara, K., S. Tone, I. Maruyama, K. Inoue, A. Katsume, H. Nuriya, H. Ohmori, J. Ohkawa, K. Taira, Y. Hoshikawa, F. Shibasaki, M. Reth, Y. Minatogawa, and M. Kohara.** 2004. Activation of the CKI-CDK-Rb-E2F pathway in full genome hepatitis C virus-expressing cells. J. Biol. Chem. **279:**14531–14541.
33. **Umehara, T., M. Sudoh, F. Yasui, C. Matsuda, Y. Hayashi, K. Chayama, and M. Kohara.** 2006. Serine palmitoyltransferase inhibitor suppresses HCV replication in a mouse model. Biochem. Biophys. Res. Commun. **346:**67–73.
34. **Wasley, A., and M. J. Alter.** 2000. Epidemiology of hepatitis C: geographic differences and temporal trends. Semin. Liver Dis. **20:**1–16.
35. **Watashi, K., N. Ishii, M. Hijikata, D. Inoue, T. Murata, Y. Miyanari, and K. Shimotohno.** 2005. Cyclophilin B is a functional regulator of hepatitis C virus RNA polymerase. Mol. Cell **19:**111–122.
36. **Weng, L., J. Du, J. Zhou, J. Ding, T. Wakita, M. Kohara, and T. Toyoda.** 2009. Modification of hepatitis C virus 1b RNA polymerase to make a highly active JFH1-type polymerase by mutation of the thumb domain. Arch. Virol. **154:**765–773.
37. **Yasuda, S., H. Kitagawa, M. Ueno, H. Ishitani, M. Fukasawa, M. Nishijima, S. Kobayashi, and K. Hanada.** 2001. A novel inhibitor of ceramide trafficking from the endoplasmic reticulum to the site of sphingomyelin synthesis. J. Biol. Chem. **276:**43994–44002.
38. **Zhong, J., P. Gastaminza, G. Cheng, S. Kapadia, T. Kato, D. R. Burton, S. F. Wieland, S. L. Uprichard, T. Wakita, and F. V. Chisari.** 2005. Robust hepatitis C virus infection in vitro. Proc. Natl. Acad. Sci. U. S. A. **102:**9294–9299.

RNA Polymerase Activity and Specific RNA Structure Are Required for Efficient HCV Replication in Cultured Cells

Asako Murayama[1☯], Leiyun Weng[2☯], Tomoko Date[1], Daisuke Akazawa[1,3], Xiao Tian[2], Tetsuro Suzuki[1], Takanobu Kato[1], Yasuhito Tanaka[4], Masashi Mizokami[5], Takaji Wakita[1]*, Tetsuya Toyoda[2]*

1 Department of Virology II, National Institute of Infectious Diseases, Tokyo, Japan, **2** Unit of Viral Genome Regulation, Key Laboratory of Molecular Virology & Immunology, Institute Pasteur of Shanghai, Chinese Academy of Sciences, Shanghai, People's Republic of China, **3** Pharmaceutical Research Lab, Toray Industries, Inc., Kanagawa, Japan, **4** Department of Clinical Molecular Informative Medicine, Nagoya City University Graduate School of Medical Sciences, Aichi, Japan, **5** Research Center for Hepatitis and Immunology, Kohnodai Hospital, International Medical Center of Japan, Chiba, Japan

Abstract

We have previously reported that the NS3 helicase (N3H) and NS5B-to-3'X (N5BX) regions are important for the efficient replication of hepatitis C virus (HCV) strain JFH-1 and viral production in HuH-7 cells. In the current study, we investigated the relationships between HCV genome replication, virus production, and the structure of N5BX. We found that the Q377R, A450S, S455N, R517K, and Y561F mutations in the NS5B region resulted in up-regulation of J6CF NS5B polymerase activity *in vitro*. However, the activation effects of these mutations on viral RNA replication and virus production with JFH-1 N3H appeared to differ. In the presence of the N3H region and 3' untranslated region (UTR) of JFH-1, A450S, R517K, and Y561F together were sufficient to confer HCV genome replication activity and virus production ability to J6CF in cultured cells. Y561F was also involved in the kissing-loop interaction between SL3.2 in the NS5B region and SL2 in the 3'X region. We next analyzed the 3' structure of HCV genome RNA. The shorter polyU/UC tracts of JFH-1 resulted in more efficient RNA replication than J6CF. Furthermore, 9458G in the JFH-1 variable region (VR) was responsible for RNA replication activity because of its RNA structures. In conclusion, N3H, high polymerase activity, enhanced kissing-loop interactions, and optimal viral RNA structure in the 3'UTR were required for J6CF replication in cultured cells.

Citation: Murayama A, Weng L, Date T, Akazawa D, Tian X, et al. (2010) RNA Polymerase Activity and Specific RNA Structure Are Required for Efficient HCV Replication in Cultured Cells. PLoS Pathog 6(4): e1000885. doi:10.1371/journal.ppat.1000885

Editor: Michael Gale Jr., University of Washington, United States of America

Received October 21, 2009; **Accepted** March 30, 2010; **Published** April 29, 2010

Funding: A.M. is supported by the Japan Health Sciences Foundation and Viral Hepatitis Research Foundation of Japan. This work was supported by grants from the Chinese Academy of Sciences (O514P51131 and KSCX1-YW-10-03), the Chinese 973 project (2009CB522504) and the Chinese National Key Project (2008ZX1000Z-14) to T.T., and a grant-in-aid for Scientific Research from the Japan Society for the Promotion of Science, from the Ministry of Health, Labor and Welfare of Japan, and from the Ministry of Education, Culture, Sports, Science and Technology and by the Research on Health Sciences Focusing on Drug Innovation from the Japan Health Sciences Foundation to T.W. The funders had no role in study design, data collection and analysis, decision to publish, or preparation of the manuscript.

Competing Interests: The authors have declared that no competing interests exist.

* E-mail: wakita@nih.go.jp (TW); ttoyoda@sibs.ac.cn (TT)

☯ These authors contributed equally to this work.

Introduction

Hepatitis C virus (HCV) contains a positive-stranded RNA genome and belongs to the *Flaviviridae* family [1]. Chronic HCV infection affects more than 130 million people worldwide [2]. The HCV RNA genome is approximately 9.6 kb in length and contains a long open reading frame that encodes a polyprotein of approximately 3,010 amino acids. This polyprotein is processed into at least 10 polypeptides by host and viral proteases [3,4]. The 5'-untranslated region (UTR) contains a highly conserved internal ribosome entry site (IRES) that is 341 nucleotides long [5]. The 3'UTR is known to contain a variable region (VR), a poly pyrimidine "U/C" (polyU/UC) tract, and a 98-base X-region (3'X tail) [6]. The second stem loop of the X region interacts with the NS5BSL3 cis-acting replication element (CRE) and may contribute to initiation of negative strand RNA synthesis [7].

JFH-1 belongs to genotype 2a and is the only strain that can efficiently replicate and produce virions in HuH-7 and HuH-7-derived cell lines [8,9,10]. When the structural protein-coding regions of the non-replicating HCV strains were fused to the non-structural protein-coding region and 3'UTR of JFH-1, replication was initiated and virions were produced in HuH-7-derived cells [10,11]. In order to analyze the mechanisms underlying the robust replication of JFH-1, we compared JFH-1 with J6CF. J6CF shares approximately 90% sequence homology with JFH-1 but does not replicate in HuH-7 cells. Analysis of JFH-1/J6CF chimeras demonstrated that the NS3 helicase-coding region (N3H) and the NS5B-to-3'X (N5BX) region of JFH-1 conferred replication activity to J6CF in HuH-7 cells [12]. Mutations in the N3H region are expected to affect helicase activity, while mutations in the NS5B-to-3'X region may affect polymerase and replication activity through secondary or higher order structures of the RNA. We have also previously reported that JFH-1-type mutations in the NS5B region enhanced genotype 1b RdRP activity *in vitro* [13]. Thus, JFH-1-type mutations in the NS5B region of J6CF are hypothesized to enhance J6CF RdRP activity. As mentioned above, the 3'UTR of the HCV genome consists of a VR, polyU/UC tracts of various lengths and a highly conserved 3'X tail. Deletion of the VR was reported to allow replication in both cultured cells [14] and in the chimpanzee [15]. The

Author Summary

Hepatitis C virus (HCV) is a major cause of chronic liver disease. Chronic HCV infection affects more than 130 million people worldwide. An efficient cell culture system is indispensable for HCV research and the development of antiviral strategies, including antiviral drugs and vaccines. Using one HCV strain, JFH-1, we have developed a novel cell culture system that, for the first time, has allowed for both the production of infectious HCV and the analysis of the HCV life cycle. To date, JFH-1 is the only HCV strain that replicates efficiently in cultured cells. Understanding the mechanisms underlying replication of JFH-1 in cultured cells is important and advantageous for the development of antiviral strategies. In the present study, we demonstrate that high polymerase activity, enhanced kissing-loop interactions between the NS5B and 3′X regions, and optimal viral RNA structure of the 3′ UTR are required for the efficient replication of JFH-1 and viral production in cultured cells. Our data provides information that will prove essential for the establishment of replication-competent variants of HCV strains that are currently replication incompetent in cultured cells. This study also contributes to a better understanding of the mechanisms underlying persistent HCV infections.

minimum length of polyU/UC tract required for replication has also been previously determined [14,16].

In the current study, we examined RNA polymerase activity and the RNA structures of the NS5B and 3′UTR that contribute to HCV replication, and determined the essential domains required for robust HCV RNA replication in cultured cells.

Materials and Methods

Cell culture

HuH-7 cells [17] and Huh-7.5.1 cells [9] were cultured at 37°C in Dulbecco's modified Eagle's medium containing 10% fetal bovine serum under 5% CO_2 conditions.

Construction of plasmids encoding a C-terminal 12xHis tagged HCV RdRP lacking 21 C-terminal amino acids

HCV JFH-1 and J6CF RdRP without the C-terminal 21 amino acid hydrophobic sequence were PCR amplified from pJFH1 [8] and pJ6CF (a kind gift from Jens Bukh) [15], respectively. Primer sequences for mutagenesis are listed in Table S1. Following digestion with *Xba*I and *Xho*I, DNA fragments were cloned into the *Nhe*I and *Xho*I sites of pET21b (Novagen, Madison, WI), resulting in pET21bHCVJFH-1RdRpwt and pET21bHCVJ6-CFRdRpwt. pET21bHCVJFH-1RdRpwt and pET21bHCVJ6-CFRdRpwt were then digested with *Xba*I and *Xho*I and the RdRP fragments cloned into the same restriction sites of pET28a, resulting in pET21(KM)JFH-1RdRpwt and pET21(KM)J6CFR-dRpwt, respectively.

Mutation analysis of J6CF and JFH-1 RdRP

JFH-1-type substitutions (S377R, A450S, S455N, R517K, and Y561F in the NS5B region; amino acid numbers are based on the AA relative numbering [18]) were introduced into J6CF RdRP and J6CF-like substitutions (S450A, N455S, K517R, F561Y, and F561I) and D318A were introduced into JFH-1 RdRP using the QuickChange II Site-Directed Mutagenesis Kit (Stratagene, La Jolla, CA). Primer sequences for mutagenesis are listed in Table S1. Sequences were confirmed by nucleotide sequencing.

Expression, purification, and *in vitro* transcription of HCV RdRP

pET21(KM)JFH-1RdRPwt, pET21(KM)J6CFRdRPwt, and their mutants were expressed with pGEX-HSP90α [13] in *Escherichia coli* Rosetta/pLysS (Novagen). RdRP was then purified as previously described [13], with the exception that protein induction was undertaken at 18°C for 4 h. *In vitro de novo* transcription was performed as described previously [13]. Briefly, following 30 min pre-incubation without ATP, CTP, or UTP, 0.1 μM HCV RdRP was incubated in 50 mM Tris/HCl (pH 8.0), 200 mM monopotassium glutamate, 3.5 mM $MnCl_2$, 1 mM DTT, 0.5 mM GTP, 50 μM ATP, 50 μM CTP, 5 μM [α-^{32}P]UTP, 0.02 μM RNA template (SL12-1S) and 100 U/ml human placental RNase inhibitor at 29°C for 90 min. [^{32}P]-RNA products were subjected to PAGE (6% gel, 8 M urea). The resulting autoradiograph was analyzed with a Typhoon trio plus image analyzer (GE Healthcare, Piscataway, NJ). The radio isotope count of 184 nt RNA product of each mutant RdRPs was measured and compared to that of JFH-1 RdRP wt in the same PAGE.

Subgenomic-replicon constructs

pSGR-J6/N3H+5BSLX-JFH1/Luc was constructed by replacement of the 5BSL-to-3′X fragment (9211 to 9678 of JFH-1) generated by PCR with the corresponding fragment of pSGR-J6/N3H+3′UTR-JFH1/Luc [12]. Constructs with substitutions in NS5B region were generated as follows; mutations were introduced by PCR-based mutagenesis and *Xho*I-*Xba*I-restricted fragments were exchanged with the corresponding fragment of pSGR-J6/N3H+5BSLX-JFH1/Luc or pSGR-J6/N3H+3′UTR-JFH1/Luc [12]. To generate the constructs used for the analyses of the 3′UTR, VR fragments (9415–9479 of JFH-1 and J6CF) or polyU/UC fragments (9480–9579 of JFH-1 and 9480–9606 of J6CF) were generated by PCR and replaced with the corresponding fragment of pSGR-J6/N3H+5BSLX-JFH1/Luc. To generate the constructs with substitutions in the VR or 3′SL2, mutations were introduced by PCR-based mutagenesis and *Sgr*AI-*Xba*I-restricted fragments were exchanged with the corresponding fragment of pSGR-J6/N3H+5BSLX-JFH1/Luc. Primer sequences for mutagenesis are listed in Table S1.

Full-length genomic HCV constructs

Plasmids used in the analysis of genomic RNA replication and core production were constructed from pJ6/N3H+N5BX-JFH1 [12] and pJ6CF [15]. pJ6/N3H+5BSLX-JFH1 was constructed by replacement of the corresponding sequence with the 5BSL-to-3′X fragment (9211 to 9678 of JFH-1) generated by PCR. pJ6/N3H+3′UTR-JFH1 was constructed by using the N3H region [*Cla*I (3929) - *Eco*T22I (5293)] and 3′UTR [*Stu*I (9415) - *Xba*I (9678)] of JFH-1 to replace the corresponding sequences of pJ6CF. Mutagenesis was performed as described above.

RNA synthesis and transfection

RNA synthesis and transfection were performed as described previously [8,12]. Briefly, plasmids were linearized with *Xba*I, treated with Mung Bean Nuclease (New England Biolabs, Ipswich, MA) and purified. Linearized, purified DNA was then used as a template for *in vitro* RNA synthesis using the MEGAscript T7 kit (Ambion, Austin, TX) in accordance with the manufacturer's instructions. Synthesized RNA was treated with DNase I (Ambion) followed by purification using ISOGEN-LS (Nippon Gene, Tokyo, Japan). The quality of the synthesized RNA was examined via agarose gel electrophoresis. Ten micrograms of *in vitro*-

synthesized RNA was used for each electroporation. Trypsinized HuH-7 cells or Huh-7.5.1 cells (3×10^6 cells) were washed with Opti-MEM I (Invitrogen, Carlsbad, CA) and resuspended in Cytomix buffer [19]. RNA was then combined with 400 µl of cell suspension and the mixture was transferred to an electroporation cuvette (Bio-Rad, Hercules, CA). The cells were then pulsed at 260 V and 950 µF using the Gene Pulser II apparatus (Bio-Rad). Transfected cells were immediately transferred to 6-well plates containing culture medium and incubated at 37°C under standard 5% CO_2 conditions.

Luciferase reporter assay

Luciferase activity of the JFH-1 subgenomic replicon and chimeras in HuH-7 cells were measured as described previously [12,20]. Briefly, 5 µg of transcribed RNA was transfected into 3×10^6 HuH-7 cells by electroporation. Transfected cells were immediately resuspended in culture medium and seeded into 6-well culture plates. Cells were then harvested at 4, 24, and 48 h after transfection and lysed with 200 µl of Cell Culture Lysis Reagent (Promega, Madison, WI). Debris was removed by centrifugation. Luciferase activity was quantified using a Lumat LB9507 luminometer (EG & G Berthold, Bad Wildbad, Germany) and a Luciferase Assay System (Promega). Assays were performed three times independently, with each value corrected for transfection efficiency as determined by measuring luciferase activity 4 h after transfection. Data are presented as relative light units (RLU).

Quantification of HCV core protein

To estimate the concentration of HCV core protein in the culture medium, we harvested supernatants at the indicated time points. The supernatant was then passed through a filter with a 0.22- µm pore size (Millipore, Bedford, MA) and subjected to the chemiluminescence enzyme immunoassay (Lumipulse II HCV core assay, Fujirebio, Tokyo, Japan) in accordance with the manufacturer's instructions.

Infection of cells with secreted HCV and determination of infectivity

Culture medium from RNA transfected cells was collected at 72 hours post-transfection. Huh7.5.1 cells were seeded at a density of $1x10^4$ cells per well in poly-*D*-lysine coated 96-well plates (CORNING, Corning, NY). On the following day, the collected culture media were serially diluted and used for inoculation of the seeded cells, and the plates were incubated for another 3 days at 37°C. The cells were fixed in methanol for 15 min at −20°C, and the infected foci were visualized by immunofluorescence as described below.

Cells were blocked for 1 hour with BlockAce (Dainippon Sumitomo Pharma, Osaka, Japan), then washed with PBS, followed by incubation with anti-core antibody at 50 µg/ml in BlockAce. After incubation for 1 hour at room temperature, the cells were washed and incubated with a 1:400 dilution of AlexaFluor 488-conjugated anti-mouse IgG (Molecular Probes, Eugene, OR) in BlockAce. The cells were then washed and examined using fluorescence microscopy (Olympus, Tokyo, Japan). Infectivity was quantified by counting the infected foci and expressed as focus forming units per milliliter (ffu/ml).

Chemicals and radio isotope

Nucleotides were purchased from GE, [α-^{32}P]UTP from New England Nuclear (Boston, MA), and human placental RNase inhibitor and restriction enzymes from TaKaRa (Shiga, Japan).

Statistical analysis

Significant differences were evaluated using the Student's *t*-test. $p<0.05$ was considered significant.

RNA secondary structure prediction

RNA secondary structure prediction was performed using Mfold software [21].

Results

As we have reported previously, the NS3 helicase and the NS5B-to-3′X regions of JFH-1 are important to confer replication competence to J6CF, a replication-incompetent strain [12]. Of these two regions, NS5B-to-3′X of JFH-1 is the most important to replication-competence. The NS5B region encodes RdRP, and the JFH-1-version of this polymerase may have high activity and be crucial to replication-competence. The requirement of 3′UTR of JFH-1 suggested that the RNA structure in this region is important for efficient genome replication. To understand the mechanisms of efficient replication of JFH-1 in HuH-7 cells, we focused on the NS5B-to-3′X region because the NS3 helicase region of JFH-1 had relatively minor effects on replication of J6CF derivatives [12]. In order to identify the important protein domains within RdRP required for efficient virus replication, we compared the RNA polymerase activity of HCV J6CF RdRP to that of JFH-1 RdRP using three assays, *in vitro* transcription with purified RdRP, *in vivo* virus RNA replication, and *in vivo* virus production. To identify the important sequences or structures in the NS5B-to-3′X region involved in efficient replication, we analyzed the effect of sequence differences in this region on replication of the viral genome.

Comparison of RNA polymerase activity *in vitro*

By comparing the sequence of RdRP of JFH-1 (GenBank Accession No. AB047639), J6CF (AF177036), other 2a strains (AB047640 – 5, AY746460, AF238481 - 5, AF169002 -5), a 1a strain (H77: AF009606), and four 1b strains (Con1: AJ238799, AB080299, AY045702, M58335), we found 14 amino acids variants unique to JFH-1 RdRP (57T, 130P, 131Q, 150A, 377R, 405I, 435V, 450S, 455N, 474M, 479H, 517K, 561F and 571S). We focused on five JFH-1-type amino acid substitutions (Q377R, A450S, S455N, R517K, and Y561F) that have been shown to increase the polymerase activity of 1b RdRP [13]. We introduced these JFH-1-type amino acid substitutions into J6CF RdRP, individually and in combination, to test their effects on polymerase activity. We also tested a J6CF RdRP variant with a R517K substitution because it was included in the J6/N3H+5BSLX-JFH1 replicon (see below), although it did not enhance the polymerase activity of 1b RdRP *in vitro* [13].

The RdRPs of HCV JFH-1 and J6CF and mutant variants were purified as indicated in the Materials and Methods and Fig. S1A. The polymerase activity of wild-type (wt) and mutant RdRPs was measured using a *de novo* transcription system (Fig. 1 and Fig. S1B). The activity of J6CF RdRP was 7.0±0.6% of that of JFH-1. Similar to results seen with 1b RdRP substitution variants, the single amino acid substitutions Q377R, A450S, S455N, R517K, and Y561F resulted in increased polymerase activity of J6CF RdRP (25.5±1.5, 27.7±1.0, 53.1±0.9, 16.9±3.5 and 16.7±2.5% of JFH-1 RdRP wt, respectively). However, combining double and triple amino acid substitutions did not demonstrate any additive or synergistic effects on the *in vitro* polymerase activity (Fig. 1).

JFH-1 RdRP variants with individual J6CF-type amino acid substitutions, including R377Q, S450A, N455S, K517R, and F561Y, were also examined *in vitro*. With the exception of N455S,

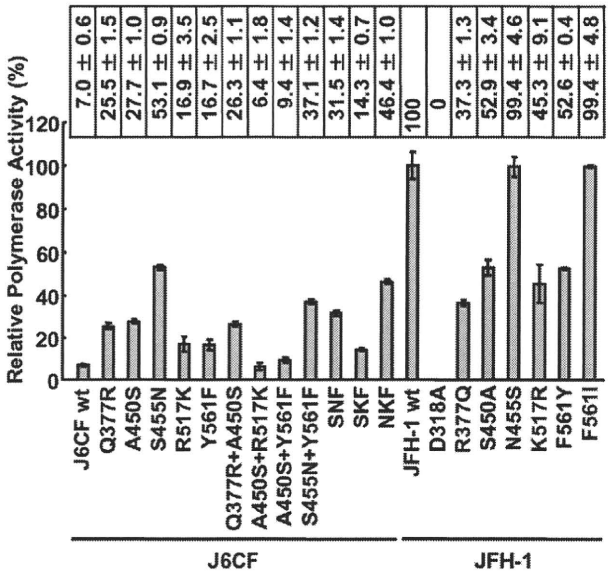

Figure 1. Relative HCV RNA polymerase activity of JFH-1 and J6CF wild-type and mutant RdRP. HCV RdRP activity was measured using the purified HCV RdRP (Fig. S1A) and the average RdRP activity and the standard deviation (error bar) relative to that of JFH-1 RdRP wt were calculated from three independent experiments (Representative gel images are shown in Fig. S1B). The relative activity values are presented above the graph. SNF, A450S+S455N+Y561F; SKF, A450S+R517K+Y561F; NKF, S455N+R517K+Y561F.
doi:10.1371/journal.ppat.1000885.g001

all other J6CF-type amino acid substitutions reduced the activity of JFH-1 RdRP, with levels ranging from 37.3 to 52.9% of the activity from wt JFH-1 RdRP (Fig. 1). The N455S variant maintained polymerase activity similar to that of JFH-1 wt. The JFH-1 D318A variant has a mutation in the active site of RdRP and showed no polymerase activity, confirming our *in vitro* transcription system.

JFH-1-type amino acid residues in the NS5B region restored the replication activity of the J6CF-based replicon

In order to test whether the JFH-1-type amino acids substitutions into the NS5B region of J6CF that enhanced polymerase activity *in vitro* enabled the replication of J6CF in cultured cells, we used the subgenomic J6CF replicon harboring the NS3 helicase region and 3′UTR of JFH-1 (J6/N3H+3′UTR-JFH1-Luc; Fig. 2A) as a reference construct. This replicon could replicate in cultured cells but exhibited less than 1% of the JFH-1 replication activity [12]. In order to test the effect of JFH-1 type amino acids on replication, we introduced the five substitutions that increased polymerase activity of J6CF RdRP *in vitro* (Q377R, A450S, S455N, R517K, and Y561F, see Fig. 2B) into the subgenomic replicon J6/N3H+3′UTR-JFH1-Luc and analyzed their effects on RNA replication. Among these JFH-1-type amino acids substitutions, Y561F was the most effective (23.2±3.5% of J6/N3H+N5BX-JFH1-Luc; Fig. 2C), while A450S, S455N, and R517K exhibited only a small effect on the replication activity (7.1±0.6%, 3.0±0.5%, and 5.5±1.0% of J6/N3H+N5BX-JFH1-Luc, respectively; Fig. 2C). The Q377R mutation demonstrated no effect on replication (Fig. 2C). We next tested the effects of Y561F in combination with each of the other substitutions. We found that A450S, S455N, and R517K mutations enhanced the replication activity of Y561F (59.1±6.1%, 43.9±6.6%, and 57.9±4.6% of J6/N3H+N5BX-JFH1-Luc, respectively; Fig. 2C). We also tested the effects of triple mutations and found that the replication activity of the SNF (A450S+S455N+Y561F) and SKF (A450S+R517K+Y561F) mutants demonstrated 86.8±6.0% and 112.2±7.9% replication activity of J6/N3H+N5BX-JFH1-Luc, respectively (Fig. 2C). In addition, we did not observe any significant differences between replicon activity of these mutants and that of J6/N3H+N5BX-JFH1-Luc. A combination of four mutations (SNKF; A450S+S455N+R517K+Y561F) resulted in similar activity as SKF (115.2±11.7% of J6/N3H+N5BX-JFH1-Luc; Fig. 2C). These results indicated that Y561F represented the most effective JFH-1-type mutation required for efficient replication, and that SKF and SNKF were sufficient to support replication activity equivalent to that of the replicon with the entire NS5B and 3′ UTR of JFH-1 (J6/N3H+N5BX-JFH1-Luc). The additive effects of the JFH-1-type NS5B substitutions on the replicon differed from results obtained with the *in vitro* polymerase activity assay.

Next, we examined whether these substitutions were sufficient for full-genome RNA replication and virus production. We used Huh-7.5.1 cells to assess virus production because Huh-7.5.1 is highly permissive for HCV propagation [9]. We found that J6/N3H+3′UTR-JFH1-Luc showed weak replication activity (Fig. 2C), and the core protein was not detectable in the culture medium of J6/N3H+3′UTR-JFH1-transfected cells (Fig. 3B). The constructs expressing A450S, S455N, or R517K substitution variants demonstrated only very low core levels in the supernatant, while the construct expressing the Y561F mutation underwent RNA replication and produced the core protein (Y561F; 15.5±3.0% of J6/N3H+N5BX-JFH1; Fig. 3B). Double mutants containing the Y561F mutation were found to produce greater amounts of core protein than the Y561F single mutant (A450S+Y561F, 57.4±3.3%; S455N+Y561F, 45.9±4.0%; and R517K+Y561F, 61.9±5.8% of J6/N3H+N5BX-JFH1; Fig. 3B). The triple mutant SNF (A450S+S455N+Y561F) produced more core protein than the double mutants (75.7±12.0% of J6/N3H+N5BX-JFH1; Fig. 3B). In addition, we observed that the core production from the SKF and SNKF mutant RNA-transfected cells was similar to the levels produced by J6/N3H+N5BX-JFH1 (111.5±8.8% and 119.0±5.1% of J6/N3H+N5BX-JFH1, respectively; Fig. 3B). We also measured infectivity of the supernatants from the mutant RNA-transfected cells at 72h after transfection (Fig. 3B). The levels of infectious titers correlated with the core levels among the tested constructs in this experiment. These results indicated that the SKF substitutions in the C-terminal region of NS5B were sufficient to elevate viral RNA replication and viral production.

Extra complementary sequence at the 5BSL3.2 kissing-loop interaction site of JFH-1 was essential for efficient replication

We observed a discrepancy between the *in vitro* RNA polymerase activity assay and the genome replication assay in the effects of the amino acid substitutions (Figs. 1 and 2C). Y561F was the most effective JFH-1-type amino acid substitution in the replication assay, while S455N was the most effective in the *in vitro* polymerase activity assay. As the kissing-loop interaction between 5BSL3.2 and 3′X are important for RNA replication and amino acid (aa) 561 encoding nucleotides are involved in the stem-loop 3.2 in the NS5B region (5BSL3.2) [7,16,22], we hypothesized that the cis-factor (genome structure) may also affect RNA replication in the cells. Thus, we constructed the subgenomic replicon J6/N3H+5BSLX-JFH1-Luc and the full genome construct J6/N3H+5BSLX-JFH1 that contained the NS3 helicase region and the 5BSL3-to-3′X region